United States Department of the Interior

Geological Survey

Preliminary Geological, Geophysical, and Biological Data from the Gorda Ridge

by

David Clague, Walter Friesen, Paula Quinterno, Lisa Morgenson,
Mark Holmes, Janet Morton, Robin Bouse, and Alice' Davis

U.S. Geological Survey
345 Middlefield Road
Menlo Park, California 94025

Prepared in Cooperation with the
U.S. Minerals Management Service

Open-File Report 84-364

INTRODUCTION

The Gorda Ridge, an oceanic spreading center with a full-spreading rate of about 5.5 cm/year, is located within 200 n. miles of the coast of northern California and southern Oregon (Figure 1). The ridge consists of three segments of ridgecrest offset by short transform fault zones or overlapping spreading centers. It is bounded to the north by the Blanco transform fault and to the south by the Mendocino fracture zone. A short chain of seamounts, named the President Jackson seamounts, trend northwesterly from a point on the ridge at about 42°N. The entire Gorda Ridge is only about 160 n. miles long and the southern 50 n. miles of the ridge is covered by turbidites. This section is called the Escanaba Trough.

Morphologically, the ridge axis is quite wide, from several to nearly 10 n. miles in width at the top of the inward facing fault scarps. The ridge axis is also unusually deep, ranging from about 3200 m to over 3800 meters. The axial graben has from about 800 to more than 1400 m of vertical relief. Numerous small seamounts flank the ridge axis from about 41°N to 42°N. To the east of the ridge axis, all but the larger seamounts are buried beneath turbidite sediment of the Astoria deep sea fan.

Previous studies of the magnetic lineations in the region show that the ridge offset near 42°N is actually a triple junction (ridge-ridge-transform), and that the spreading rates north and south of this triple junction are distinct. To the north the full spreading rate is about 5.5 cm/yr, while to the south it is only about 2.3 cm/yr (Atwater and Mudie, 1973; Riddihough, 1980). The more southerly ridge offset, located near 41.5°N, is characterized by swarms of small earthquakes (Northrup et al., 1968) and may also be a ridge-ridge-transform triple junction with up to 0.2 cm/yr left-lateral offset (Riddihough, 1980).

Atwater and Mudie (1973) gave a detailed description of the topography, sediment distribution and magnetization of the northern section of the Escanaba Trough. They concluded that the central rift valley resulted from large scale normal faulting that broke the surface into long narrow tilted steps parallel to the spreading center. They described flat-lying sediment in the Escanaba Trough and noted that sediment also occurred on top of some of the fault blocks bounding the valley, thus implying that the fault blocks were uplifted to form the valley walls as they moved outwards from the spreading axis.

DATA INCLUDED IN THIS REPORT

During 1980 to 1983, the U.S. Geological Survey conducted geological or geophysical surveys of the Gorda Ridge during four cruises. The first cruise, L12-80-WF, collected several days of underway geophysical data near the northern end of the Escanaba Trough. The second cruise, L11-81-NC, collected underway geophysical data, including multichannel seismic data, over the southern and central Escanaba Trough. These two cruises were conducted on the U.S.G.S. ship R/V S.P. LEE. The next cruise, KK1-83-NP, collected SeaMARC II sidescan imaging and underway geophysical data from the Blanco Transform to the northern end of the Escanaba Trough. The final cruise KK2-83-NP, collected bottom samples at 15 of 17 dredge sites. The latter two cruises were conducted on the University of Hawaii ship R/V Kana Keoki under sponsorship of the Minerals Management Service.

This report shows the tracklines for the underway geophysical data from these cruises and presents the single-channel seismic reflection profiles from

cruise KK1-83-NP. The additional data, including the SeaMARC II data, will be released as soon as final navigation and processing of the imaging data are complete.

Much of this report describes the samples recovered during cruise KK2-83-NP which departed Eureka, California on October 8, 1983, and returned to Eureka on October 13, 1983. Samples collected during this cruise include fresh pillow basalt, hydrothermally altered pillow basalt, hydrothermal deposits from the spreading axis, hydrogenous Mn-oxide deposits from a small seamount, sediment samples, and biological specimens (both attached to rocks and in the sediment samples). Later sections of this report will present the data and discuss the implications for hydrothermal activity along the Gorda Ridge. The dredge locations and tracks of included seismic profiles are shown in Figures 2 and 3. The dredge locations and depths are given in Table 1. Dredge 5 was empty because the dredge bag was ripped open. Dredge 8 was lost.

UNDERWAY GEOPHYSICAL DATA

The general bathymetry, earthquake epicenters, locations of sediment samples and heat flow stations, magnetics, gravity, and seismic reflection and refraction studies in the Gorda Ridge area are compiled in map form by Wilde et al., (1978). New underway data collected by the USGS during our four cruises between 1980 and 1983 are available from the National Geophysical Data Center (NGDC) in Boulder, Colorado. The available data are indicated in Table 2 and the tracklines for cruises L12-80-WF, L11-81-NC, and KK2-83-NP are shown in Figure 2. An integrated suite of underway geophysical data was collected along 2300 km of track over the Blanco Fracture Zone and the northern two-thirds of Gorda Ridge during cruise KK1-83-NP of the R/V Kana Keoki between 27 September and 6 October 1983. The instrument systems used included SeaMARC II side-scan sonar, single channel air gun seismic reflection, gravity, magnetics, and 3.5 kHz bathymetry. Positioning control was accomplished using a satellite-Omega receiver and a separate Loran C receiver with a Cesium beam time standard. A track chart constructed from the satellite fix information is shown in Figure 3.

SeaMARC II (Seafloor Mapping And Remote Characterization) is an intermediate range side-scan sonar system capable of obtaining high quality acoustic imagery over a 10-km wide swath at a ship speed of 7.5 knots. The tracklines were spaced at an 8.5-km interval during the survey to ensure overlap of the image fields along adjacent tracks. Acoustic phase data are also collected by the SeaMARC II system. These data can be processed after the cruise to produce a bathymetric contour map at a 100-m contour interval. This bathymetric map can then be used in conjunction with the side-scan acoustic imagery in the interpretation of structural, geological, and morphological features.

The SeaMARC II data set is presently being processed and merged with the Loran C navigation base. This will permit construction of a fully corrected side-scan image mosaic of the area surveyed. The synoptically gathered bathymetric data will be contoured and displayed on the same position base. Selected side-scan images from the survey are shown in Figure 7.

Seismic reflection data were collected using 40 in^3 and 120 in^3 air guns as a sound source. The shot repetition rate was 8 seconds; the data were processed in two overlapping frequency bands and displayed on standard dry paper facsimile recorders. Record sections (low frequency) across the Gorda Ridge and Blanco Fracture Zone are shown in Figure 4.

The gravity and magnetics data collected along the tracklines will be merged with the Loran C navigation and displayed in contour form at the same scale as the side-scan imagery and bathymetry. All of the geophysical data will be submitted to the NOAA/NGDC after the final processing is completed and the Loran C data base has been edited and finalized.

SINGLE CHANNEL SEISMIC REFLECTION DATA

The air gun reflection lines obtained across Gorda Ridge on cruise KK1-83-NP have been assembled in Figure 4 to show the characteristics of the ridge at approximately 8.5-km intervals from the Blanco Fracture Zone to the northern end of Escanaba Trough. The figure is composed of four panels, arranged from north to south; line numbers are shown in Figure 3.

The morphology of the ridge and its prominent axial valley show considerable variation from track to track. In some places the valley floor is 10 to 20 km wide with an irregular surface (lines 77, 80, and 89); in other locations the central depression is a sharp notch (lines 99, 101). Maximum depth over the ridge axis is along line 101 (3800 m). The depth to the valley floor appears to vary systematically manner. The shallowest crossings are along lines 83, 95, and 107; these lines are 85 km apart.

Several of the crossings (lines 71, 77, 83, 87, 95, and 103) show small volcanic cones or domes in or near the valley axis. The flat floor and layered reflectors shown in the axial valley along line 79 suggest that sheet flows may have issued from the base of the western valley wall.

Maximum relief of the central depression and its flanking walls reaches almost 2000 m along lines 73 and 79. The irregular topography of the ridge flanks are due to long linear fractures which are parallel or subparallel to the ridge axis. Some of these scarps can be traced on the preliminary SeaMARC imagery for more than 150 km.

MULTICHANNEL SEISMIC REFLECTION PROFILES

Three 24-channel seismic reflection profiles were obtained along and across the Escanaba Trough in September 1981 during cruise L11-81-NC. The profiles were collected aboard the U.S. Geological Survey research vessel S.P. Lee using 34.9-l, 2.000-psi airgun array. Two profiles cross the ridge at lat. 41°N (line 114) and lat. 40°30'N (line 118), and a third profile runs along the ridge axis from lat. 41°30'N to south of the Mendocino Fracture Zone (Figure 2). Preliminary brute stacks of lines 114 and 118 are shown in Figures 5 and 6, respectively. Although these preliminary records are noisy, several observations can be made about the Escanaba Trough.

Along line 114, the spreading axis is marked by a 10-km wide valley flanked by ridges which rise 1200 to 1300m above the valley floor (Figure 5). A thick layer of sediment (approximately 0.5 seconds, two-way) covers the axial valley floor. The ridge flanks are also mostly covered by sediment, thicker on the eastern flank than the western flank. An outward-tilted, sediment-covered block on the eastern flank could represent a former axial valley floor. Several small extensional faults cut the upper part of the sediments of the axial valley. Disruption of the deeper sediments, especially prevalent near the center of the axial valley, could represent volcanic sills or dikes intruding the sediments.

There is no surface expression of a ridge on line 118, which crosses the southern end of the Escanaba Trough (Figure 6). A shallow graben about 50m deep and 5km wide and several smaller extensional faults mark the spreading

axis. The sediment cover at the axis is considerably thicker along line 118 than it is to the north. Although it is difficult to trace the sediment-basement contact, it appears that the sediment cover is thickest at the axis and thins to both the east and west. The sediment layer at the spreading axis is greater than 1 second thick (two-way).

The presence of faults which cut the surficial sediments demonstrate that the Escanaba Trough is undergoing active extension. These faults could provide both the recharge and discharge paths for hydrothermal systems.

SeaMARC II SIDE-SCAN IMAGERY

The tracklines of the side-scan sonar data collected on cruise KK1-83-NP are shown in Figure 3. Selected images of the SeaMARC II data set are shown in Figure 7. Locations for each of these examples are shown in Figure 3.

Figure 7-1 shows an area of about 100 km^2 over the axial graben. Note the linear fractures on the inner valley walls. The height of the scarps is on the order of 30 to 50 m. The higher reflectivity of the valley floor with respect to the walls is probably due to pillow basalt texture.

The records shown in Figures 7-2 and 7-3 show opposing segments of the axial graben at a major right - lateral offset of the ridge axis. The dark pattern in Figure 7-2 is thought to represent an exposed (fresh?) volcanic surface. Note the large truncated cone 1 km in diameter in the upper right and the strong white shadow cast by a narrow ridge in the upper left. The linear feature marked A is identified in both Figure 7-2 and 7-3.

Figure 7-3 is an image across the ridge axis just south of that shown in Figure 7-2; the image fields overlap (Fig. 3). The area covered by Figure 7-3 is about 200 km^2. Crustal movements at this offset have fractured a truncated cone (lower left center) into three segments with left-lateral slip along the fractures. In the lower center a ribbon-like flow has been extruded from a small cone.

PETROLOGY OF THE LAVAS

Mid-ocean ridge basalt was recovered in all 15 successful dredges. The samples have been subdivided into flow units based on hand-sample characteristics including phenocryst mineralogy, apparent age based on palagonite thickness, morphology of the fragments, and on microprobe glass compositions. All the recovered samples are pillow fragments; no lobate or sheet-flow fragments were recovered. A number of the lavas have thick glassy rims and very thin to no palagonite. Most of the lavas are plagioclase phyric or plagioclase and olivine phyric, but a few flow units are aphyric. Clinopyroxene phenocrysts have been identified in only a few samples. Table 3 summarizes the descriptions of the flow units and describes the alteration observed.

Glass chips from 42 lava samples have been analyzed for major and minor elements using a 9-channel electron microprobe. The results are listed in Table 4 on a normalized basis. All the samples are low-K_2O mid-ocean ridge tholeiite including the dredge 17 sample from a seamount to the east of the spreading axis. The lavas are variable in composition, ranging from magnesium numbers ($100xMg/(Mg+Fe^{2+})$) of 53 to 69. Many of the flow units identified on the basis of hand sample characteristics have identical glass compositions indicating that individual flow units are quite variable in phenocryst mineralogy and flow form, or suggesting that eruptions at any given location along the ridge can be quite uniform through time.

The lava compositions include primitive melts that have fractionated little in sub-axial magma chambers (dredge 4) and ferrobasalt that has fractionated and possibly mixed with other melts in sub-axial magma chambers (dredges 3, 6, and 16). Note that none of the ferrobasalt is as evolved as that from the Juan de Fuca Ridge. Fractionation of these lavas in sub-axial magma chambers implies that the magma chambers and their associated hydrothermal systems are relatively long-lived. There is no apparent systematic along-strike variation in the composition of the lavas. Detailed isotopic and trace element studies are underway that should clarify the origin and evolution of the dredged lavas.

Most of the dredges were on the bottom for only short distances, yet many dredges recovered a number of flow units. This observation suggests that individual flows along much of the Gorda Ridge are small in areal extent and therefore in volume.

Our results are consistent with previous studies of lavas dredged from the Gorda Ridge (Kay et al., 1970; Wakeham, 1978). However, most of the samples dredged prior to cruise KK2-83-NP are either poorly located (the saamples described by Kay et al., 1970) or are older lavas dredged from the seamounts flanking the ridge axis. Prior to our work, only three dredges by Oregon State University (OSU) cruise W7605B had sucessfully sampled the axis of the spreading center. The OSU dredge locations, as well as those described by Kay et al., (1970) and one dredge on the President Jackson seamounts are shown on Figure 2. All the previously analyzed samples fall within the range of compositions given in Table 4 except those from President Jackson seamount which include both low-K_2O mid-ocean ridge basalt and alkalic basalt (Melson et al., 1977).

HYDROGENOUS AND HYDROTHERMAL DEPOSITS AND ALTERATION OF THE LAVAS

Many of the lava samples have thin coatings of hydrogenous Mn-oxides (generally δMnO_2, but also birnessite and todorokite) and display incipient to developed palagonitization of the glassy rims. Other deposits and alteration products appear to have a higher temperature hydrothermal origin. The most common alteration along fractures in the lavas is smectite, but albite, quartz, and Mn- and Fe-oxides are also nearly ubiquitous. Other phases of hydrothermal origin include chlorite, gypsum, barite, talc, boehmite, kaolinite, K-feldspar(?), and sulfide phases.

Talc is positively identified in dredges 7 and 13, and tentatively identified in dredges 3, 6, and 9. Talc precipitates as Si-rich hydrothermal fluid mixes with Mg-rich ambient seawater; it has been described from hydrothermal deposits in the Gulf of California (Lonsdale et al., 1980) and has been identified as a hydrothermal phase on lava from the Juan de Fuca Ridge (Eaby and Clague, 1982). Chlorite is abundant as an alteration product along fractures in the lavas from dredges 3, 4, 6, 7, 9, 11, 12, 13, 14, and 17. Chlorite apparently forms from the reaction of basaltic glass and hydrothermal fluid at elevated temperatures.

Gypsum, barite and the sulfide phases discussed below appear to be relatively high temperature precipitates from hydrothermal fluids as they progressively mix with ambient seawater. The occurrence of boehmite (AlO(OH)) is surprising considering that Al is not readily mobilized by hydrothermal fluids. However, amorphous Si-Al "gels" have been described from sulfide samples from both 21°N on the East Pacific Rise (Oudin, 1982) and the Juan de Fuca Ridge (Koski et al., 1984). These occurrences suggest that under certain conditions, Al is mobilized and transported by hydrothermal fluid.

Albite on these samples generally occurs as a white to grey deposit on the spalled glass surface and in fractures in the glassy rinds of pillow fragments. The hydrothermal fluid contains abundant Si and Na, but as in the case of boehmite, the source of the Al is unclear. It is possible that the Al is derived from the basaltic glass.

Quartz is generally present with chlorite in fractures. Disordered kaolinite with minor K-feldspar(?) occurs as a white coating on glass in dredge 14.

Dredge 16, in addition to the hydrothermal nontronite-Mn-oxide samples described below, contains altered sulfide as well. Many of the large pillow basalt fragments are coated on fractures with a yellowish material that smells of sulfur. X-ray diffraction reveals that pyrite is present in some of this material. We interpret these deposits to be altered sulfide similar to that described below.

In summary, most of the lavas recovered underwent low-to-moderate temperature alteration and deposition of hydrothermal phases. Dredges 9 and 10 recovered the least altered lavas.

MASSIVE LOW-TEMPERATURE HYDROTHERMAL DEPOSITS

Dredge 16 recovered about 100 kg of hydrotheraml nontronite and associated Fe and Mn oxides. Descriptions of ten subsamples are given in Table 5 and partial chemical analyses of samples of this deposit are presented in Table 6. Low-temperature hydrothermal nontronite deposits have been described from a number of other locations including the Galapagos spreading center (Corliss et al., 1978), the Gulf of Aden (Cann et al., 1977), the Explorer Ridge (Grill et al., 1981) and the Juan de Fuca Ridge (Murnane and Clague, 1983). The Gorda Ridge nontronite deposit has an upper Mn-oxide layer, a zone of Fe-oxides, and an inner zone of bedded to aureolic nontronite and hydrothermally altered detrital sediment. Unlike the other described deposits, the Gorda deposit is riddled by worm tubes indicating the presence of abundant fauna at the time the deposit was forming or subsequent to its formation. No worms were recovered with the hydrothermal deposit indicating that this location is not a site of present day hydrothermal activity.

The chemical data given in Table 6 demonstrate the low abundances of Zn, Cu, Ni, Pb, and Co present. Ni and Mo show a strong positive correlation with Mn concentration. However, all the analyzed samples are notably low in Co, Ni, and Cu. The Mn-oxides phases present in the outer crust include birnessite, natrobirnessite, todorokite, manjiroite (?), and manganite (?). The bulk of the deposit is composed of interbedded nontronite and detrital sediment composed of illite, smectite, chlorite, quartz and plagioclase. The high Fe samples do not contain any well-crystallized Fe-oxide phase; amorphous $Fe(OH)_3$ probably constitutes the bulk of these samples.

Detailed studies of the nontronite and Mn-oxides are in progress; these studies should clarify the temperatures at which these hydrothermal deposits formed. Similar deposits elsewhere formed at 19-57°C (Murnane and Clague, 1983). These temperatures are well below the temperatures at which most sulfide deposition occurs (~250°C; Oudin, 1982) at submarine hydrothermal vents. The nontronite/Mn-oxide deposits represent a low-temperature hydrothermal deposit that could stratigraphically overlie, or could occur adjacent to, higher temperature sulfide deposits. In any case, hydrothermal activity persisted at this location for an extended period of time. The longevity of the hydrothermal discharge is evidenced by the interlayering of hydrothermal and detrital sediment.

SULFIDE MINERALIZATION

Sulfide mineralization is present in a handful of samples from dredge 7. None of the hydrothermal sulfide is massive. Two sulfide assemblages are present. In the first type, pyrite and pyrrhotite occur with a Mn-Fe-Ca-carbonate (manganosiderite?) lining fractures in pillow basalt fragments. Pyrrhotite occurs as 30μm flat hexagonal plates (Fig. 9a) set in a clay matrix (Fig. 9b). Figure 9c is a close-up of the manganosiderite(?) shown in the upper right hand corner of Figure 9a. Pyrite in these samples is present as <10μm to ~30μm cubes that are partially corroded (Figures 9d,e).

The second sulfide assemblage in dredge 7 samples consists of pyrite and sphalerite with barite also present. The sulfide-sulfate minerals line open channels inside contorted basaltic fragments. Figure 9f shows euhedral barite crystals projecting into the open channel. Figure 9g shows cubic pyrite as 30μm crystals and as tiny ~2μm crystals growing on clay minerals. Figure 9h shows the entire assemblage of barite, sphalerite, and euhedral and strongly corroded pyrite, and Figure 9i is a close-up of the barite in Figure 9h.

Mn-OXIDES CRUST RECOVERED IN DREDGE 17

Dredge 17 sampled a small off-axis seamount and recovered relatively fresh pillow basalt encrusted by brown hydrogenous Mn-oxides up to 1 cm thick. X-ray diffraction shows the crusts are composed of vernadite todorokite, birnessite(?), and abundant smectite. The bulk Mn-oxide crust was analyzed for Mn, Fe, Co, Ni, and Cu by atomic absorption spectrophotometry. The concentrations determined are: Mn = 14.59 wt%, Fe = 15.07 wt%, Co = 0.26 wt%, Ni - 0.21 wt%, and Cu = 230 ppm. The crust has similar Co, but far lower Ni and Cu contents than deep sea abyssal nodules.

SEDIMENT SAMPLES

Sediment samples were collected in a small (4 x 15") pipe dredge dragged behind the large chain bag dredge. In addition, large chunks of thick pasty gray sediment were recovered in several rock dredges. The pipe dredge used was lined with a canvas sample bag; we refer to these as "sock" samples. Descriptions of the sediment samples are given in Table 7 and mineralogy and bulk chemical analyses determined by atomic absorption spectrophotometry are given in Tables 8 and 9, respectively, for the <0.063 mm size-fraction. Twenty-one sediment samples were prepared for determination of their clay mineralogy (15 sock samples, 6 from dredges). The procedures are outlined in the footnotes to Table 8. The relative percentages of smectite, illite, and chlorite were determined by X-ray diffraction on glycollated samples. The results in Table 8 are reproducable to within 5%; however the actual percentages may be biased due to uncertainty in the weighing factors employed.

Most of the samples reacted very little when soaked in the Morgan's solution and peroxide indicating very low calcium carbonate and organic carbon contents. Samples D11(MUD), D17(MUD), and D17(SOCK) reacted the most strongly.

The sediments range in color from a light olive gray to dusky yellow brown. Regardless of color, all the sediments are composed of similar proportions of illite, chlorite, and smectite, and variable amounts of quartz and plagioclase. The variation in color is apparently due solely to the addition of small (<1.5 wt%) amounts of manganese oxides of probable hydrothermal origin. Iron concentration is constant through all the samples,

as are Zn, Ni, and Cu. Co, Pb, and Mo were below detection levels of 50, 50, and 100 ppm in all but the light-colored sediment from dredge 7 which contained 270 ppm Pb.

The sock samples that are brown in color generally contain abundant glass fragments and agglutinated benthic foraminifera. Those that are gray in color generally have few glass fragments and agglutinated benthic foraminifera but do contain abundant radiolaria and diatoms, commonly clumped together in fecal pellets. We interpret the brown sediments to be very thin deposits on the basalt surface that are brown due to the addition of hydrothermal Mn-oxides. The abundant benthic foraminifers probably reflect proximity to hydrothermal vents. Iron carried in hydrothermal vent waters precipitates relatively near the vents, but Mn is carried some distance from the vents due to its precipitation at higher eH and slow nucleation kinetics. The brown muds recovered from the Gorda Ridge are enriched in Mn but not in Fe, which suggests that they were deposited relatively far from hydrothermal vents.

GORDA RIDGE FORAMINIFERS

Benthic foraminifers are the most abundant fauna recovered from the Gorda Ridge area. Sediment samples were wet sieved and the >0.065 mm portion of sediment was examined for foraminifers. Samples D13 (SOCK) and D14 (SOCK) contained mostly glass fragments, the other nineteen sediment samples contain abundant agglutinated and calcareous benthic foraminifers; agglutinated tests are composed of volcanic glass fragments, mineral grains, sponge spicules or other detrital particles. Planktonic foraminifers are present in most samples, but are generally less abundant. Thirty-five agglutinated genera and 32 calcareous genera have been identified (Table 10); these forms are typical of deep sea environments. References used for identification are Barker (1960), Cushman (1910, 1911), and Loeblich and Tappan (1964). The agglutinating fauna includes many large tubular forms such as Rhabdammina, Bathysiphon, Rhizammina, Bottellina, and Hyperammina. Some of these, such as Rhabdammina irregularis are attached to the surface of pillow basalt fragments. When these forms are abundant, the rock appears to be nearly covered by a tangled network of branching tubes--some even extending into cracks in the rock. Uniserial lituolids, including several species of Reophax and coiled lituolids, such as Trochamminoides, Haplophragmoides, and Trochammina are also abundant. Trochammina was found attached to some basalt fragments.

Although some calcareous forms are present, agglutinating assemblages are dominant. This is to be expected as most of the samples were collected from water depths greater than 3000m where bottom waters are usually undersaturated in calcium carbonate. Plates 2-4 show some of the species present in the samples.

Table 11 summarizes the characteristics of the foraminiferal fauna for each sample: benthic and planktonic foraminiferal abundance (number of individuals); diversity (number of species); preservation state; composition of the tests; and size (whether or not specimens greater than 1.0mm are present). Because dredges were used to obtain all samples, a true measure of foraminiferal abundance and diversity is not possible. Furthermore, due to the large amount of material and limited amount of time, the data in Table 11 are estimates, but are useful for comparing one sample with another.

Abundance and Diversity

Foraminifers are common to abundant in all but 5 samples (Table 11); in most samples benthics outnumber planktonics in both volume and number of individuals. D17 (SOCK) and D17 (MUD) are exceptions; planktonics are abundant in both. These samples are from much shallower water than the others (1700m compared to >3000m).

The diversity (number of species) was estimated to be high (>20 species) in the majority of samples.

The source of food for these abundant deep-sea faunas is uncertain; benthic foraminifers are known to eat unicellular algae, small animals, dissolved and colloidal organic molecules, organic rich grains (including fecal pellets), and bacteria (Haynes, 1981). However, it is not known, at present, which of these elements are a source of food for the Gorda Ridge faunas.

Test Composition and Size

Large agglutinating benthic foraminifers dominate the faunas in most samples (Table 11). Agglutinating foraminifers are known to use a variety of materials to construct their tests. Some select only quartz grains, others use sponge spicules or even tests of other foraminifers. An unusual feature of the foraminifers from Gorda Ridge area is the common use of large angular fragments of volcanic glass in test construction, particularly among certain species of Rhabdammina, Reophax, Psammosphaera, and Trochamminoides (Plates 2-4). The resulting tests are interesting, but the irregular shapes produced by the use of large, angular grains makes comparison with previously described species difficult, and therefore, identification uncertain. For example, Flint (1899) described Psammosphaera parva as a usually spherical, thin-walled form composed of fine sand with cement filling in smoothly the interstices and angles of the sand grains; the test is often built around a long sponge spicule. The Gorda Ridge samples contain specimens of Psammosphaera mostly composed of large angular volcanic glass fragments with a generally spherically-shaped but somewhat irregular test. The sponge spicule is lacking, but is replaced by a blade-shaped piece of volcanic glass (Plate 2, figure 3).

Preservation

Most samples are fairly well preserved; e.g., the specimens are fresh looking, many are unbroken and not heavily stained with iron coatings. Some calcareous specimens show signs of dissolution and boring. D17 (sock), one of the less well preserved samples has several broken specimens of Cassidulina and Ehrenbergina, some of which are filled by glauconite.

OTHER MICROORGANISMS FROM GORDA RIDGE

Smear slides were prepared from the <0.063mm sediment fractions, and 25 fields of view were counted using a light microscope at 250x to determine the number of diatoms, radiolarians, and silicoflagellates. Fifty fields of view were counted for coccoliths. Table 12 summarizes the abundances of diatoms, radiolarians, silicoflagellates and coccoliths in the sediment samples. Although radiolarians were absent in some smear slides, they were observed in the coarser(>0.063mm) portions of these samples which were used for

foraminiferal analysis. To give a more accurate picture of radiolarian abundance, the coarser fractions were scanned and an estimate of radiolarian abundance included in Table 12.

LARGER FAUNA FROM THE GORDA RIDGE

In addition to the benthic foraminifers and planktonic microorganisms described above, the dredges from the Gorda Ridge recovered a wide variety of other fauna. Most of these samples have been examined at the Smithsonian Institution by a group of biologists. In addition, we have found a number of additional specimens in the sieved fractions of the mud samples. By far the most abundant fauna is siliceous sponges which occur in dredges 2, 7, 12, and 14. Sponge spicules are present in all the mud samples but are particularly abundant in the muds from dredges 1, 3, 7, and 14. Anemones of the genus Actinauge occur attached to sponge fragments in dredge 2; other anemones of the family Zoanthidea encase sponge spicules in dredge 12. Black corals belonging to the order Antipatharian occur in dredges 7 and 14. Worm tubes are especially abundant in dredge 16, but also occur in dredges 1, 2, and 10. An unidentified polychete worm was recovered in dredge 10. Dredge 11 contained an unidentified stalked crinoid from the family Hyocrinidae and dredge 14 contained the base of an unidentified crinoid. Dredge 3 recovered a specimen of a brittle starfish Dytastes Gilbert Fisher. Dredge 10 recovered an unidentified Octopoda and dredge 16 recovered a small unidentified bony fish. Pelecypoda fragments were recovered in dredges 4, 10 and 14, and an unidentified gastropod in dredge 15. Dredge 2 recovered 4 chitinous inarticulate Brachiopoda.

It is worth noting that a great number of these specimens were recovered in the small pipe dredge with sediment and that many of the others were found only due to extremely thorough examination of the entire dredge contents. None of the fauna are known to occur specifically around hydrothermal vents but the general abundance of fauna indicates an abundance of food that may reflect proximity to vents. In particular, the abundance of agglutinated benthic foraminifers appears to reflect proximity to hydrothermal vents as they are most abundant in those muds showing chemical evidence for a hydrothermal component.

DISCUSSION

The data presented in this report indicate that hydrothermal activity is widespread along the axis of the northern two-thirds of the Gorda Ridge. Nearly all the evidence is indicative of rather low-temperature hydrothermal activity or even the interaction of seawater and hot rock on the seafloor, with the exception of the sparse sulfides, sulfates, and talc deposits recovered in dredge 7. At this site, high temperature hydrothermal fluids capable of precipitating sulfides apparently debouch on the seabed. We have no data that would suggest how long-lived these hydrothermal systems may be, if they are presently active, or whether massive sulfide deposits occur that are similar to those described from the East Pacific Rise at 21°N (RISE Project Group, 1980; CYAMEX Scientific Team 1979, 1981), the Galapagos Spreading Center (Law et al., 1981), and the Juan de Fuca Ridge (Normark et al., 1982, 1983). Biological density, particularly of benthic foraminifers, indicate more widespread hydrothermal acitvity. Chemical analyses of hydrothermal nontronite and associated Mn-oxides, of Mn-oxide crusts (recovered in dredge 16 from a small off-axis seamount), and of brown muds

containing variable small hydrothermal components all show low concentrations of Cu, Zn, Ni, Co, and Pb; Mn and Fe are the only metals present in significant concentrations.

The geophysical data demonstrate that the axial valley of the northern two-thirds of the Gorda Ridge is deep, narrow, and rough. We anticipate that detailed camera surveys, used so successfully to locate massive sulfide deposits on the East Pacific Rise and Juan de Fuca Ridge, will be difficult to perform in such rough terrain. We suspect that the Escanaba Trough, where very little geological/geophysical surveying has been done, may prove to be the most promising part of the Gorda Ridge for sulfide exploration. This conclusion is based on relative ease of exploration in the flat sediment-filled trough (using deep-tow side-scan techniques) and that the sediment could serve as a source of metals in addition to the underlying basaltic crust. Many of the large ophiolite-hosted massive sulfide deposits are now thought to have formed in back-arc basins, and some are hosted by volcanogenic sediment. Although the Gorda Ridge is not situated in a back-arc basin, the Escanaba Trough is filled with volcanogenic sediment that is geochemically similar to that shed into back-arc basins from the active volcanic arcs. Thus, although the tectonic setting of the Gorda Ridge is not identical to that inferred for large ophiolite-hosted sulfide deposits, the physical similarities between the Escanaba Trough and back-arc basins suggests that the Escanaba Trough warrants further exploration.

ACKNOWLEDGEMENTS

This report was completed quickly due to a true team effort. Others whose help was essential to completion of this report in a timely manner include R. Oscarson for help with the SEM, Wendy Bohrson for help with plates and figures, Carol Hirozawa for help with foraminifers, and Kay McDaniel for typing. The helpful support of the crew of the R/V Kana Keoki insured the success of the sampling cruise. We are particularly indebted to Jackie Eaby who helped organize and run the KK2-83-NP cruise. We are grateful to John Pogeta, Jr., U.S.G.S., and David L. Pawsen, Smithsonian Institution for their work on the macrofauna

REFERENCES

Atwater, T., and J.D. Mudie, 1973, Detailed near-bottom geophysical study of the Gorda Rise. Jour. Geophys. Res., 78, p. 8665-8686.

Barker, R.W., 1960, Taxonomic Notes on the species figured by H.B. Brady in his Report on the Foraminifera Dredged by H.M.S. CHALLENGER During the Years 1873-1876: Soc. Econ. Paleontologists and Mineralogists. Spec.Publ. no. 9, 238 p.

Cann, J.R., C.K. Winter, R.G. Pritchard, 1977, A hydrothermal deposit from the floor of the Gulf of Aden. Mineral Mag., 41, p. 193-199.

Corliss, J.B., M. Lyle, J. Dymond, and K. Crane, 1978, The chemistry of hydrothermal mounds near the Galapagos Rift. Earth Planet Sci. Letts., 40, p. 12-24.

Cushman, J.A., 1910, A monograph of the foraminifera of the north Pacific Ocean, Pt. I Astrorhizidae and Lituolidae: U.S. Nat. Museum Bull. 71, 134 p.

Cushman, J.A., 1911, A monograph of the foraminifera of the north Pacific Ocean, Pt. II Textulariidae, U.S. Nat. Museum Bull. 71, 108 p.

CYAMEX Scientific Team, 1979, Massive deep-sea sulfide ore deposits discovered on the East Pacific Rise. Nature, 277, p. 523-528.

CYAMEX Scientific Team, 1981, First manned submersible dives on the East Pacific Rise at 21°N (Project RITA): General results. Marine Geophys. Res., 4, p. 345-379.

Eaby, J.S., and D.A. Clague, 1982, Preliminary descriptions of basalt from the southern Juan de Fuca Ridge. U.S. Geol. Surv. Open-File Report 82-200C.

Flint, J.M., 1899, Recent foraminifera. A descriptive catalogue of specimans dredged by the U.S. Fish Commission Steamer Albatross. U.S. Nat. Mus. Am. Rept. (1897), Washington, D.C., U.S.A., pt. 1, p. 268.

Grill, E.V., R.L. Chase, R.D. MacDonald, J.W. Murray, 1981, A hydrothermal deposit from Explorer Ridge in the Northeast Pacific Ocean. Earth Planet. Sci. Lett., 52, p. 142-150.

Haynes, J.R., 1981, Foraminifera: N.Y., John Wiley, 433 p.

Kay, R., N.J., Hubbard, and P.W. Gast, 1970, Chemical characteristics and origin of oceanic ridge volcanic rocks, Jour. Geophys. Res., 75, p. 1585-1613.

Koski, R.A., D.A. Clague, and E. Oudin, 1984, Mineralogy and chemistry of massive sulfide deposits from the Juan de Fuca Ridge. Geol. Soc. Am. Bull. (in press).

Law, S., A. Malahoff, R. Embley, and D. Fornari, 1981, Massive polymetallic sulfides of the Galapagos Rift. EOS (Am. Geophys. Union Trans.), 62, p. 1027.

Loeblich, A.R. and H. Tappan, 1964, Treatise on Invertebrate Paleontology, Pt. C, Protista 2: Univ. Kansas Press, 900 p.

Lonsdale, P.F., J.L. Bischoff, V.M. Burns, M. Kastner, and R.E. Sweeney, 1980, A high temperature hydrothermal deposit on the seabed at a Gulf of California spreading center. Earth. Planet. Sci. Lett., 49, p. 8-20.

Melson, W.G., G.R. Byerly, J.S. Nelen, T. O'Hearn, T.L. Wright, and T. Vallier, 1977, A catalog of the major element chemistry of abyssal volcanic glasses. Smithsonian Contrib. Earth Sci., 19, p. 31-60.

Murnane, R., and D.A. Clague, 1983, Nontronite from a low-temperature hydrothermal system on the Juan de Fuca Ridge. Earth Planet. Sci. Lett., 65, p. 343-352.

Normark, W.R., J.E. Lupton, J.W. Murray, J.R. Delaney, R.A. Koski, D.A. Clague, J.L. Morton, and H.P. Johnson, 1982, Polymetallic sulfide

deposits and water column tracers of active hydrothermal vents on the southern Juan de Fuca Ridge. Marine Technology Soc. Jour., 16, p. 46-53.

Normark, W.R., J.L. Morton, R.A. Koski, D.A. Clague, and J.R. Delaney, 1983, Active hydrothermal vents and sulfide deposits on the southern Juan de Fuca Ridge. Geology, 11, p. 158-163

Northrup, J., H.W. Menard, and F.K. Duennebier, 1968, Seismic and bathymetric evidence of a fracture zone on the Gorda Ridge. Science, 161, p. 688-690.

Oudin, E., 1982, Etudes mineralogique et geochemique des depots sulfures sois-marins actuals de la ride est-pacifique (21°N): Documents du Bureau de Recherches Geologiques et Minieres 25, 241 p.

Riddihough, R.P., 1980, Gorda plate motions from magnetic anomaly analysis. Earth Planet. Sci. Lett., 51, p. 163-170.

RISE Project Group, 1980, East Pacific Rise: Hot springs and geophysical experiments, science, 207, p. 1421-1433.

Wakeham, S.E., 1978, Petrochemical patterns in young pillow basalts dredged from the Juan de Fuca and Gorda Ridges. Unpub. MSc. thesis, Oregon State University, 95 p.

Wilde, P., T.E. Chase, M.L. Holmes, W.R. Normark, J.A. Thomas, D.S. McCulloch, and L.D. Kulm, 1978, Oceanographic data off northern California - southern Oregon, 40-43° North including the Gorda Deep-sea fan. Lawrence Berkeley Laboratory Publication 251.

Table 1. Dredge Locations on Gorda Ridge-Cruise KK2-83-NP

Station Number	Start of Dredge			End of Dredge			Recovery
	Lat.(n)	Long.(w)	Depth(m)	Lat.(n)	Long.(w)	Depth(m)	
1	42°56.99'	126°37.26'	3285	42°56.26'	126°37.69'	3175	150 Kg of basalt
2	42°54.42'	126°40.92'	3180	42°54.46'	126°39.74	3250	<50 Kg of basalt
3	42°51.56'	126°41.87'	3165	42°49.84'	126°42.06'	3150	200 Kg of basalt
4	42°45.58'	126°45.47'	3060	42°45.21'	126°45.92'	3385	200 Kg of basalt
5	42°43.05'	126°45.91'	3060	42°44.83'	126°45.18'	2980	Empty, dredge bag broken
6	42°33.26'	126°.50.55'	3615	42°35.28'	126°51.58'	2960	300 Kg of basalt
7	42°28.30'	126°53.82'	3775	42°28.55'	126°52.83'	3540	300 Kg of basalt
8	42°21.37'	127°03.81'	3110	42°22.81'	127°04.14'	3245	Lost dredge
9	42°14.33'	127°04.83'	3045	42°15.43'	127°04.44'	3050	500 Kg of basalt
10	42°23.10'	127°03.83'	3260	42°21.87'	127°04.24'	3200	<1 Kg of mud + glass chips
11	42°06.94'	127°08.89'	3105	42°07.41'	127°10.00'	3110	400 Kg of basalt
12	42°02.32'	127°10.13'	3425	42°01.87'	127°09.04'	---	200 Kg of basalt
13	41°48.16'	127°10.27'	3310	41°48.25'	127°09.89'	3240	150 Kg of basalt
14	41°41.49'	127°13.69'	3260	41°41.94'	127°14.07	3300	200 Kg of basalt
15	41°36.50'	127°18.11'	3390	41°37.54'	127°18.40'	3420	<50 Kg of basalt
16	41°30.96'	127°27.62'	3320	41°31.56'	127°27.07'	3360	350 Kg of basalt + hydrothermal nontronite
17	41°27.65'	127°13.63'	1700	41°27.68'	127°13.44'	1705	150 Kg of Mn-encrusted basalt

Table 2. Available Underway Geophysical Data

	Cruise			
	L11-81-NP	L12-80-WF	KK1-83-NP*	KK2-83-NP
3.5kHz or 12kHz Bathymetry	X	X	X	X
Magnetics	X	X	X	
Gravity	X		X	
Single Channel Seismic Data		X	X	
Multichannel Seismic Data	X			
SeaMARC II Side-Scan Data			X	

All data available on magnetic tape from NGDC except that for cruise KK1-83-NP for which final navigation is still being processed. As soon as processing is complete, data will be sent to NGDC.

Table 3. Hand sample petrography of variolitic pillow basalts dredged from Gorda Ridge off California and Oregon, northeast Pacific Ocean.

Dredge Number	Lithologic Type No.	Color (fresh break)	Phenocrysts Mineralogy	Phenocrysts Percent	Phenocrysts Size (mm)	Glass Thickness (mm)	Glass Surface Texture	Glass Palagonite	Vesicles	Alteration and Surface Deposits Mineralogy	Remarks
1	1	Dark gray (N3)	Plagioclase Olivine	<5 <1	±3 ±1	<10	Ropy to smooth to striatad	None to incipient	Round to irregular, <20%, ±1 mm diam.	Albite Nontronite(?) Chlorite Goethite(?) Hematite(?)	Phenocrysts are most abundant in-and-just-below the glassy rind, decreasing downward as the crystallinity of the rock increases; texture becomes dikty-taxitic at depth; glass is altered along fractures; numerous fractures in the rocks display colorsd metal oxide deposits; many pieces are pillow lava blister fragments or glassy protuberances.
2	1	Medium derk gray (N4) to derk gray (N3)	Plagioclase Olivine	1-2 <1	1-2 <1	0-2	(Spalled)	None	Round to irregular, <1%, <1 mm diam.	Goethite(?) Hematite(?)	Plagioclase and olivine as glomerocrysts; iron oxides coat fracture faces locally and fill veinlets; most are small fragments with no glassy surfaces, perhaps pieces of pillow interior as the groundmass is quite crystallins; alteration is incipient and adherent clay is tan to brown in contrast to the olive gray color of dredged bottom-mud.
	2	Black (N1)	Plagioclase Olivine	15 <1	2 <1	5+	Ropy	Incipient	Round, <1%, <1 mm diam.	Alhite(?) Chlorite(?)	Plagioclase is glomerophyric with olivine; glassy rind is perlitic with palagonitization developed in surficial fractures; hydrothermal deposits line fractures which penetrate the pillow fragments.
	3	Black (N1) to medium derk gray (N4)	A p h y r i c			<20	(Spalled)	?	None	δ-MnO_2(?) Hematite(?) Goethite(?)	Appears to be very fresh basalt; drsdge recovery was small and the pebble-sized fragments are quite subrounded for the most part; varioles quickly become abundant at shallow depth in the glassy rind.
3	1	Dark gray (N3)	Plagioclase Olivine	±1 <1	1 <1	<10	Striated ropy	Incipient	Round, ±2%, <1 mm diam.	Chlorite Albite Quartz Talc(?) Todorokite(?) Gypsum(?) Nontronite(?) Jarosite(?) Goethite(?) Hematite(?) δ-MnO_2(?)	Plagioclase occure as phenocrysts, or rarely, as glomerocrysts with olivine; glass quickly becomes variolitic below the original surface, progressing downward through variolitic holocrystalline in the pillow interior to a vuggy, open-textured rock at depth; frectures in the glass ere often albitized and fractures within the pillow are lined with hydrothermal phases.
	2	Black (N1)	Plagioclase Olivine	15+ <1	±2 <1	±10	Ropy	None	Round, <1%, <1 mm diam.	None	Plagioclase occure as phenocrysts and as glomerocrysts (rarely with olivine); glass is remarkably fresh, with almost no evidence of alteration (this lithology is composed of spalled glass fragments bearing no sample of the underlying pillow basalt).
	3	Black (N1)	Plagioclase	±4	±1	±10	Ropy	Incipient to developed	Round, ±4%, ±1 mm diam.	δ-MnO_2(?)	Plagioclase occurs as single, slender phenocrysts, quite different from the flat spars and thick rods of the prsvious lithologies; glass displays more advanced palagonitization, especially in surface cracks (this lithology also is composed of spalled glass fragmente, with no samples of underlying pillow basalt).
	4	Black (N1)	Plagioclase Olivine	±3 ±1	±1 <1	±10	Ropy	Established	Round, ±4%, ±1 mm diam.	Albite(?) δ-MnO_2(?)	Plagioclase occurs as slender, acicular phenocrysts or as glomerocrysts (less frequently with olivine); original glass surface is extensively palagonitized and bears a mangenese-iron deposit up to 1 mm thick; fractures within the glass are whitened by albitization.
4	1	Dark gray (N3)	Plagioclase Olivine	<1 <1	±1 <1	<10	Ropy to "bread-crust"	Incipient to developed (in cracks)	Round to irregular, <1%, <1 mm diam.; some cylindrical to several cm	Quartz Chlorite Alhite(?) Smectite δ-MnO_2(?) Goethite Gypsum(?) Chlorophaeite Hematite(?) Todorokite(?)	Rare plagioclase and olivine glomerocrysts, olivine usually more or less altered to chlorophaeite; every surface of these pillow fragments is coated with chlorophaeite which often penetrates ±1 mm into the underlying rock; hematite(?) and todorokite(?) form a petchy coating over the chlorophaeite; glass is rare, albitized(?) along fractures, with palagonite (or goethite?) developed in surface cracks.
	2	Dark gray (N4)	Plagioclase Olivine	5 2	±3 1	3+	(Spalled)	None	Round, ±1%, <1 mm diam., progressing downward to an open texture	Chlorite(?) Hematite(?)	Plagioclase and olivine glomerocrysts; olivine is not altered to chlorophaeite as in the previous lithology; texture becomes diktytaxitic to vuggy 2-3 cm below the glassy rind, which is as plagioclase-olivine phyric as the more crystalline part of the pillow.
5		NO RECOVERY									

Table 3 (continued).

Dredge Number	Lithologic Type No.	Color (fresh break)	Phenocrysts Mineralogy	Phenocrysts Percent	Phenocrysts Size (mm)	Glass Thickness (mm)	Glass Surface Texture	Glass Palagonite	Vesicles	Alteration and Surface Deposits Mineralogy	Remarks
6	1	Grayish-black (N2) to medium gray (N5)	A p h y r i c			10	Rough ropy	Incipient	Round, <5%, abundance and size increasing downward from glassy rind	Quartz Chlorite Smectite Goethite Birnessite δ-MnO_2(?) Albite Talc(?) Hematite(?) Todorokite(?) Jarosite(?) Nontronite(?)	No apparent phenocrysts; variolitic texture is well-developed; large drainout cavities and flat and tubular vesicles are abundant and up to 10 cm in diam.; brightly-colored hydrothermal phases are abundant on fracture faces.
	2	Grayish-black (N2)	Plagioclase Olivine	10 3	5 1	10	Ropy	Established	Round, <1%, <1 mm diam., to irregular, up to 2 mm diam. at depth	Quartz Chlorite Smectite Albite(?) Barite(?) δ-MnO_2(?) Goethite(?) Hematite(?) Jarosite(?) Nontronite(?)	Plagioclase and olivine glomerocrysts, more or less consistently abundant from glassy rind through pillow interior; glassy rind displays infrequent patches of albitization along fractures.
	3	Grayish-black (N2)	Plagioclase Olivine	<1 <1	±2 ±1	±3	Smooth	Incipient	Round, ±1%, ±1 mm diam.	Albite Todorokite(?) Hematite(?) δ-MnO_2(?)	Extremely rare plagioclase and olivine phenocrysts; very glassy with incipient to developed variolitic texture in numerous protuberances; rare albitization along fractures; dusting of iron and manganese oxides on original glass surfaces.
	4	Dark gray (N3)	Plagioclase Olivine	±5 ±2	1 1	±6	Smooth ropy	Incipient	Irregular to round, ±1%, ±1 mm diam. sometimes filled with chlorophaeite	Albite(?) δ-MnO_2(?) Hematite(?) Todorokite(?)	Plagioclase phenocrysts and glomerocrysts with olivine, decreasing sharply in abundance about 10 cm below the glassy rind, but maintaining the same dimensions; large flat and tubular vesicles display abundant lava stalactites, upper surfaces of the vesicles dotted with biota and dusted with black, sooty δ-MnO_2(?); glass is albitized along fractures.
7	1	Grayish-black (N2) to dark gray (N3) to medium dark gray (N4)	Plagioclase Olivine	<1 <1	±2 ±1	±10	Smooth ropy	None	Round to irregular, ±1%, ±1 mm diam., often lined with chlorophaeite	Albite Talc Smectite Chlorite Quartz Pyrite Barite Calcite Hematite(?) Todorokite(?) Goethite(?) Nontronite(?) Chlorophaeite Jarosite(?)	Plagioclase and olivine occur rarely as phenocrysts in and just below the glassy rind; texture quickly becomes variolitic, progressing rapidly downward in the pillow from a glassy exterior to a spongy, diktytaxitic holocrystalline interior; glassy exteriors are often developed into convoluted septal forms and protuberances; palagonite, if ever developed, has been superseded by hydrothermal alteration: most surfaces are coated with unctuous, talc-like material or brightly-colored metal oxides and clay minerals; albitization has taken place in most glassy surfaces; one sample bears a tubular channel lined first with hydrothermal clays and then overcoated with minute euhedra of pyrite, berite, sphalerite, and chlorite; minute pyrrhotite euhedra were found coating an adjacent fracture face.
	2	Dark gray (N3)	Plagioclase Olivine	<<1 <<1	±1 ±1	±10	Ropy	Destroyed	Round to irregular, <5%, <1 mm diam.; also, large flat vesicles ±2 cm below glassy rind	Quartz Albite Chlorite Smectite Talc Goethite(?) Hematite(?) Todorokite(?) δ-MnO_2(?) Montronite(?)	Rare glomerocrysts of plagioclase and olivine in and just below the glassy rind; vesicle content increases with depth in the pillow, and the shape changes from round to irregular; texture is uniformly variolitic to at least 20 cm below the glassy rind; all surfaces are more-or-less intensely altered hydrothermally and coated with metal oxides; glass surfaces are albitized.
	3	Medium dark gray (N4) to dark gray (N3)	Plagioclase Olivine	±5 ±5	±3 ±3	2+	Ropy? (mostly spalled)	Incipient?	Irregular to round, <1 mm diam. (abundance varies greatly)	Todokite(?) Jarosite(?) Chlorophesite	Plagioclase occurs as phenocrysts and as glomerocrysts with olivine with abundances more-or-less constant throughout the pillow; vesicles, initially round, quickly become irregular with depth, increasing in abundance until a spongy, open texture is developed in the pillow interior; fracture faces display abundant hydrothermal deposits, including metal oxides and clay minerals; chlorophaeite alteration proceeds ±1 mm into the enclosing host rock from fracture faces.
	4	Grayish-black (N2) to dark gray to medium dark grey (N4)	Plagioclase Olivine	±3 ±1	±1 ±1	±5	Striated	Incipient	Round, <5%, <1 mm diam., (abundance varies greatly)	Albite(?) Jarosite(?) Montronite(?) Chlorite(?) Todorokite(?)	Plagioclase occurs as phenocrysts and as glomerocrysts with olivine almost exclusively below the glassy rind; texture progresses inward from variolitic glass to variolitic holocrystalline pillow interior; all surfaces display abundant evidence of hydrothermal activity: glass is albitized along fractures and on surfaces, and fracture faces are coated with brightly-colored metal oxides and clay minerals; a very rare, dust-like deposit of unaltered pyrrhotite euhedra on a tight, protected fracture face was discovered grading into orange iron oxide and dark green nontronite(?)

Table 3 (continued).

Dredge Number	Lithologic Type No.	Color (fresh break)	Phenocrysts Mineralogy	Phenocrysts Percent	Phenocrysts Size (mm)	Glass Thickness (mm)	Glass Surface Texture	Glass Palagonite	Vesicles	Alteration and Surface Deposits Mineralogy	Remarks
8		NO RECOVERY									
9	1	Black (N1) to dark gray (N3)	Plagioclase Olivine	±35 <1	±4 ±1	±10	Striated	Incipient to developed	Round, <1-50%, <1 mm diam.	None	Plagioclase occure as single (often up to 1.5 cm diam.) phenocyrsts, also as glomerocrysts with olivine; (most abundant in and just below the glassy rind); texture varies from vitrophyric to variolitic hyalopilitic; vesicles increase in abundance and size until the pillow interior finally becomes scoriaceous; this specimen and its associated fragments represent a "trapdoor pillow"; original surface of glass displays expansion texture; very little evidence of hydrothermal activity observed.
	2	Black (N1) to medium dark gray (N4)	Plagioclase Olivine	2-5 <<1	1-4 <1	2-9	Smooth to ropy	Incipient (rare-mostly spalled)	Round to irregular, 1-10%, ±1 mm diam.	Albite Smectite Clorite Talc(?) Chlorophaeite δ-MnO_2(?) Hematite(?) Nontronite(?)	Plagioclase occurs as phenocrysts, and as plagioclase ±olivine glomerocrysts (rock is essentially plagioclase-phyric only); texture is vitrophyric (glassy rind) and becomes quickly and consistently variolitic hyelopilitic below the rind; vesicle content sparse in the first 10 cm below the glassy rind, becoming abundant at depth, finally yielding a subscorieceous, open texture; hydrothermal deposits are sparing; zone of chlorophaeitic alteration extends ±2 mm into the rock from fracture facee (dark greenieh-grey color).
10	1	Black (N1)	Aphyric			(not preserved)	?	?	?	None	Entire dredge recovery consists of 285 g of light olive-gray (5Y5/2) ooze with discoid lumps of more compact, burrowed material of the same, but slightly lighter color and (probably) composition; the unconsolidated mud is set with basaltic glase chips, benthonic foraminifers, and loose plagioclase and olivine crystal fragments.
11	1	Black (N1) to dark gray (N3)	Plagioclase Olivine	±2 <1	±1 ±1	±10	Smooth to ropy (mostly spalled)	Incipient?	Round to irregular, ±1%, <1mm diam.	Quartz Smectite Birnessite Chlorite(?) δ-MnO_2(?) Todorokite(?) Nontronite(?)	Plagioclase and olivine glomerocrysts; texture renges downward from variolitic hyaline through variolitic hyalopilitic to variolitic holocrystalline; fracture faces and veinlets bear deposits of greenish-yellow hydrothermal clay and black, powdery manganese oxide.
	2	Black (N1) to grayieh-black (N2) to dark gray (N3)	Plagioclase	<1	<1	±10	Ropy to knobby	Incipient	Round, 1-5%, ±1 mm diam., also large flat vesiclee or drainouts	Quartz Albite Smectite Chlorite Birnessite Todorokite Nontronite(?) Goethite(?) δ-MnO_2(?)	Plagioclase appears rarely as small phenocryets; texture varies from holohyaline to hyaline variolitic in the glaeey rind to veriolitic hyalopilitic through variolitic holocryatalline downward in the main mass of the rock; abundant evidence of hydrothermal activity: glase is surficially whitened-to-grayed by albitization(?), most surfeces are coated with colored clay minerals and metal oxides (dark brown vernadite? on surface of glass, black, powdery todorokite? [curiouely] on upper surfecee of lerge flat vesicles, drsinout cavities, and blister cavities); pseudomorphe of goethite? after pyrite? and pyrrhotite? obaerved in aome cavities.
12	1	Black (N1)	Aphyric			(all glass)	Smooth swell-and-swele to smooth ropy	None to incipient	Round, <1%, ±1 mm diam.	Hematite(?)	Spalled aphyric basaltic glass and protuberances - glass is remarkably fresh, with only incipient palagonitization in perlitic fractures; evidence for hydrothermal activity is ecarce (brownish-red stains only on some pieces).
	2	Dark gray (N3)	Plagioclase Olivine	<1 <1	±1 ±1	10-40	Smooth (swell-and-ewale) to ropy and breadcruet-like	Established (up to 0.5 mm thick)	Irregular, up to 5%, <<1 mm diam.	Albite Smectite Chlorite Goethite(?) Hematite(?)	Essentially an aphyric rock with rare plagioclaee and olivine phenocrysts and microphenocryste; texture varies from variolitic hyaline (glassy rind) downward through variolitic holocrystalline, with a distinct holomicrovariolitic zone ±5 mm thick just below the glassy rind; glass rind is exceptionally thick, with well-preserved originel surfacee and a variety of surface textures over small areae; rare plagioclaae and olivine xenocrysts(?) observed and also e few, rare olivine and plagioclaee or clinopyroxene and plagioclaae glomerocryste; several pillow buds or protuberances obeerved still attached to pillow fragments; hydrothermal deposits abundant: white talcoae to porcellaneous albitization(?) of original glass surfaces and internal fractures, veinlets and fracture faces lined with albite(?) and colorful metal oxides.
13	1	Dark gray (N3)	Aphyric			15-30	Smooth ropy to rough "bread-cruet"-like	Incipient to developed	Round, <1%, ±1 mm diam.	Quartz Albite Chlorite Smectite Talc Boehmite Gypsum δ-MnO_2(?) Goethite(?) Hematite(?) Nontronite(?) Todorokite(?)	Texture varies from holohyaline (glassy rind) through variolitic hyalopilitic to variolitic holocrystalline, with sinuous segregations of plagioclase and olivine microcrystals between the varioles ±20 cm below the glassy rind; hydrothermal activity ie well-developed on fracture faces and in veinlets: layers ±1 mm thick of talcoae-to-porcellaneous white materiel and spotty, thin deposits of brightly-colored metal oxides.

Table 3 (continued).

Dredge Number	Lithologic Type No.	Color (fresh break)	Phenocrysts Mineralogy	Phenocrysts Percent	Phenocrysts Size (mm)	Glass Thickness (mm)	Glass Surface Texture	Glass Palagonite	Vesicles	Alteration and Surface Deposits Mineralogy	Remarks
13	2	Dark gray (N3)	Plagioclase Olivine	<<1 <<1	±2 <1	1+	Rough striated (mostly spalled)	Developed	Irregular, <<1%, (upper 10 cm) to spongy (lower 10 cm), (size and abundance increase greatly with depth)	Albite(?) Goethite(?) Hematite(?) Nontronite(?)	Similar to the previous lithology, but palagonite is more developed, manganese and iron oxide deposits coat surfaces, glass surface texture differs, alteration is less pronounced, vesicle shape, content, and distribution differ (numerous 0.5-3 cm diam. flat vesicles are abundant just below the glassy rind, also, with coatings on their upper surfaces composed of δ-MnO_2(?) and hematite(?).
14	1	Black (N1) to dark gray (N3)	Plagioclase Olivine	<<1 <<1	±2 ±1	5-30	Smooth, swell-and-swale, ropy, striated	Very incipient(?) to established	Round to irregular, percentage variable; vuggy at depth; some lined with chlorite(?)	Albite Smectite Chlorite Kaolinite Quartz Natrobirnessite Gypsum(?) K-feldspar(?) Goethite(?) Jarosite(?) Nontronite(?) Todorokite(?) Hematite(?) δ-MnO_2(?)	Plagioclase and olivine occur as rare phenocrysts; texture varies from holohyaline (glassy rind) through variolitic to variolitic holocrystalline; pillow lavas are often contorted, convoluted, with development of many protuberances; vesicles and phenocrysts more abundant in glassy rind; evidence of hydrothermal activity along fracture faces where concentric bands of metal oxide and clay mineral deposits appear with goethite(?) outermost and nontronite(?) innermost; in other samples the interior texture is diktytaxitic to vuggy pegmatoid (euhedral plagioclase crystals, segregations of altered olivine granules); and the vesicle abundances increase rapidly with depth below glassy rind yielding a spongy texture at depth; huge flat vesicles or drain-out cavities apparent 3-10 cm below the glassy rind; abundant goethite(?) haloes around central whitened (albitized?) areas on fracture faces; heavy, ubiquitous coatings of vernadite(?) on most surfaces.
15	1	Black (N1) to dark gray (N3)	Olivine	±1	<1	10+	Smooth to finely striated (mostly spalled)	Incipient	Round to irregular, <1%, ±1 mm diam., often lined with chlorite(?) or celadonite(?)	Goethite Hematite Nontronite Albite Quartz Smectite Chlorite Boehmite Talc(?) Maghemite(?) Manjiroite Natrobirnessite δ-MnO_2 α-Cristobelite Todorokite Clinoptilolite(?) Erionite(?)	Virtually aphyric except for rare microphenocrysts of olivine; texture is mostly hyaline variolitic and the samples consist mostly of broken glassy protuberances and curious knobby, warty septarian forms - centers of protuberances contain irregular gas cavities, sometimes yielding small zones of spongy, variolitic holocrystalline texture, with sinuous segregations of olivine granules around varioles; hydrothermal deposits are ubiquitous; most fracture surfaces are coated with pistachio-green-to-mustard-yellow clay minerals, often admixed with bright reddish-brown metal oxides; albitization(?) of fractures in glassy rinds; most surfaces coated with gray-white clay material.
16	1	Black (N1) to grayish-black (N2) to dark gray (N3)	Plagioclase	±20	±3	±10	Striated "bread-crust"	Incipient to developed	Round, <1%, <1 mm diam.	Albite Smectite Goethite(?) Alunite(?)	Plagioclase occurs as single phenocrysts (up to 5 mm diam.) or as glomerocrysts; glass appears to be fresher than in Lithology 2 and contains no surface deposits; texture is markedly different from Lithology 2 in that it is non-variolitic.
	2	Black (N1) to grayish-black (N4) to dark gray (N3)	Plagioclase Olivine Clino-pyroxene	5-20 ±2 <<1	±2 <1 <1	30-40	Striated "bread-crust"	Developed	Round, 1-10%, ±1 mm diam.	Albite Hematite Goethite Lepidocrocite(?) Nontronite β-Cristobalite(?) Celadonite(?) Gypsum(?) Sulphur(?) Alunite(?) Jarosite(?) Todorokite(?) Chlorite(?)	Plagioclase occurs both as phenocrysts (up to 5 mm diam.), and as glomerocrysts with olivine, one small (<1 mm diam.) emerald green clinopyroxene occurs as a glomerocryst with plagioclase and olivine; phenocryst abundances decrease rapidly with depth below the glassy rind, but olivine abundance increases with depth; texture varies from vitrophyric (glassy rind), through hyaline variolitic (zone 3-4 cm thick below glassy rind) to variolitic holocrystalline; vesicles increase with depth until a spongy, final vuggy, pegmatoid texture is developed at the center; hydrothermal deposits on fracture faces are striking: concentric bands of brightly-colored metal oxides, sulphates(?), clay minerals, and sulphur(?) on every interior surface, progressing inward from just below the glassy rind to the central vuggy zone.

Table 3 (continued).

Dredge Number	Lithologic Type No.	Color (fresh break)	Phenocrysts Mineralogy	Phenocrysts Percent	Phenocrysts Size (mm)	Glass Thickness (mm)	Glass Surface Texture	Glass Palagonite	Vesicles	Alteration and Surface Deposits Mineralogy	Remarks
1?	1	Dark gray (N3)	Plagioclase Olivine	±6 ±2	±3 ±1	±10	(not exposed)	Established (±0.5 mm thick)	Round to irregular, ±6%, <<1 mm diam.	Quartz Albite Smectite Goethite Chlorite Todorokite Birnessite(?) Amphibole Barite Butlerite(?) Celadonite α-Cristobalite β-Cristobalite δ-MnO_2(?) Jarosite Natrobirnessite	Plagioclase and olivine occur both as single phenocrysts (up to 4 mm diam.) and as glomerocrysts; texture varies from vitrophyric (glassy rind) to hyaline variolitic (just below glassy rind) to intergranular at depth; most pieces are small pillow fragments partially to totally sheathed with thick ferromanganese/smectite deposits (distinctly stratified, with interlayered δ-MnO_2, goethite, and smectite, soft, brittle, highly porous, ranging in color from moderate brown (5YR3/4) to dusky yellowish-brown (10YR2/2) to brownish-black (5YR2/1), with a warty, knobby surface frequently scoured and polished in spots); fracture faces are coated generally with buff-white, smectite, locally with colored metal oxides and pale greenish-yellow to lilac clay minerals; (one sample is a water-logged andesitic pumice-ball erratic).

Table 4. NORMALIZED GLASS ANALYSES OF GORDA RIDGE BASALTS

Flow Unit	Sample Number	SiO_2	Al_2O_3	FeO	MnO	MgO	CaO	Na_2O	K_2O	P_2O_5	TiO_2	SO_3
1	D1-21	51.1	15.4	9.61	0.19	7.57	11.2	2.65	0.15	0.20	1.62	0.29
1	D1-31	50.8	15.5	9.84	0.21	7.45	11.2	2.75	0.15	0.22	1.59	0.28
1	D1-12	50.3	15.5	9.66	0.20	7.44	11.7	2.89	0.15	0.22	1.62	0.35
1	D1-8	51.0	15.0	9.89	0.20	7.41	11.6	2.61	0.14	0.21	1.64	0.32
1	D2-3	50.6	15.1	9.93	0.21	7.60	11.9	2.62	0.09	0.17	1.60	0.25
2	D2-6	51.0	14.4	9.51	0.20	7.52	12.3	2.72	0.18	0.18	1.43	0.27
3	D2-5	51.1	15.1	9.80	0.19	7.27	11.4	2.84	0.13	0.20	1.75	0.32
1	D3-4c	51.2	15.0	9.36	0.21	7.46	12.0	2.68	0.17	0.19	1.49	0.26
1	D3-1	51.1	15.2	9.19	0.21	7.44	12.0	2.74	0.16	0.17	1.46	0.27
1	D3-4a	50.8	15.5	9.16	0.20	7.35	12.0	2.89	0.18	0.16	1.48	0.32
1	D3-6	50.9	14.9	9.24	0.18	7.34	12.4	2.86	0.18	0.19	1.49	0.33
2	D3-4b	50.7	14.9	9.28	0.19	7.33	12.5	2.89	0.19	0.17	1.49	0.36
5	D3-4	50.5	14.1	11.1	0.22	6.42	11.7	3.07	0.21	0.27	2.14	0.37
1	D4-15*	50.3	16.7	7.99	0.16	8.83	12.2	2.54	0.05	0.09	0.97	0.23
1	D4-8a	50.3	16.4	8.01	0.17	8.90	12.3	2.57	0.04	0.07	1.00	0.23
2	D4-5*	50.1	16.1	8.47	0.18	8.39	12.4	2.73	0.09	0.12	1.17	0.25
3	D6-18	51.0	14.2	10.7	0.22	7.41	11.0	2.87	0.16	0.21	1.94	0.30
1	D6-12	50.1	14.7	10.7	0.21	7.40	11.3	2.92	0.16	0.21	2.05	0.35
2	D6-4	50.8	15.1	10.1	0.20	7.26	11.4	2.69	0.13	0.18	1.81	0.32
4	D6-9*	50.8	15.1	10.1	0.22	7.16	11.5	2.75	0.14	0.21	1.76	0.30
3	D7-12*	49.9	15.6	9.78	0.21	7.89	12.0	2.65	0.09	0.16	1.43	0.29
2	D7-4	50.1	15.6	9.70	0.20	7.57	11.7	2.76	0.22	0.21	1.73	0.32
1	D7-8	51.1	15.3	9.37	0.19	7.40	11.9	2.71	0.17	0.18	1.43	0.27
1	D9-1	50.3	15.7	9.43	0.19	8.23	12.1	2.33	0.07	0.12	1.29	0.30
2	D9-2b	50.2	15.5	9.92	0.20	7.84	11.9	2.46	0.09	0.15	1.45	0.31
2	D9-3	50.0	15.1	10.1	0.21	7.66	12.3	2.64	0.09	0.11	1.49	0.33
1	D10-1	50.6	14.5	10.6	0.22	7.12	12.2	2.57	0.11	0.16	1.64	0.36
1	D11-9	50.3	15.4	9.28	0.20	8.24	12.11	2.63	0.08	0.11	1.39	0.29
2	D11-8	50.6	15.3	9.98	0.19	7.77	11.3	2.65	0.11	0.17	1.66	0.33
1	D12-2	51.0	14.5	10.3	0.20	7.94	11.1	2.74	0.10	0.15	1.68	0.33
2	D12-1	50.0	14.9	10.5	0.21	7.25	11.8	2.84	0.12	0.19	1.76	0.40
1	D13-11	50.6	15.5	9.44	0.20	8.18	12.0	2.43	0.09	0.12	1.25	0.25
1	D13-12*	50.4	15.4	9.30	0.19	8.06	12.3	2.55	0.10	0.12	1.30	0.32
1	D14-8	50.1	15.7	9.66	0.18	8.24	11.6	2.45	0.10	0.15	1.42	0.30
1	D14-13	50.3	15.5	9.77	0.21	8.16	11.6	2.53	0.11	0.14	1.42	0.24
1	D14-2	50.0	15.4	9.67	0.19	8.05	11.9	2.71	0.11	0.15	1.45	0.36
1	D14-18	49.5	15.9	9.56	0.20	7.96	12.1	2.72	0.11	0.14	1.44	0.34
1	D15-1	50.9	15.1	10.3	0.21	7.48	11.1	2.72	0.11	0.18	1.69	0.32
1	D16-3	50.1	15.8	9.71	0.20	7.36	11.5	3.00	0.14	0.16	1.67	0.34
2	D16-1	50.7	14.6	10.9	0.22	6.88	11.4	2.66	0.26	0.19	1.90	0.35
2	D16-2	50.5	14.0	11.0	0.21	6.78	11.9	2.63	0.27	0.25	1.97	0.37
1	D17-10	50.7	15.7	9.62	0.21	7.42	11.5	2.76	0.19	0.16	1.50	0.24

*Analysis listed is average of two separate analyses
Analysts: D.A. Clague and Alice' Davis

Table 5. Descriptions of nontronite-Mn-oxide hydrothermal deposits recovered in Dredge 16.

Sample	Lithology	Color	Consolidation	XRD Mineralogy	Bedding	Bioturbation	Remarks
A	Umberous manganese crust	Brownish-black (5YR2/1)	Punky, porous	Birnessite Natrobirnessite Manjiroite(?) Todorokite Quartz	Distinctly bedded	Partial penetration by worm tubes	Forms lower umberous manganese crust on hydrothermal clay/hydrothermally altered detrital sediment/oxidized sulphide(?) deposit. Gypsum(?) present.
B	Iron ochre	Light brown (5YR5/6) to moderate brown (5YR4/4) and (5YR3/4)	Crumby to pasty	Amorphous [$Fe(OH)_3$?] Smectite (Nontronite?) Coquimbite? (trace)	Bedded	Intense penetration by worm tubes	Forms (usually) layer just below punky lower, brownish-black manganese crust; may have been a deposit of pyrite; zone of abundant iron-oxide worm tubes. Gypsum(?) present.
C	Hydrothermal clay	Greenish-black (5GY2/1)	Crumby to indurated	Nontronite	Bedded to aureolic	Peripheral to and penetrated by worm tubes	Seems to form mainly around the worm tubes which penetrate it and other deposits; often capped by iron ochre deposit; often forms distinct homogeneous beds.
D	Dense, crystalline manganese crust	Dark gray (N3) to grayish-black (N2)	Tough to brittle, indurated	Todorokite Natrobirnessite Birnessite Manganite(?) Manjiroite(?) Quartz	Distinctly bedded	Not detected	Forms the ultimate capping layer of manganese crust over the other sediment layers; it is dark gray and metalloidal to grayish-black and velvety, with a botryoidal, accretionary texture; it varies in density and tenacity (some develops shrinkage cracks on exposure to air); commonly displays a rough, warty, powdery, uppermost surface.
E	Consolidated detrital sediment	Pale olive (10Y6/2)	Dense paste	Smectite Chlorite Illite Quartz Plagioclase	Often thick, massive	Abundant to intense penetration by worm tubes	Probably the most abundant of the interlayered sediment types within the deposit; site of vigorous penetration by many different types of worms.
F	Punky manganese deposit	Dark olive gray (5Y3/1) to grayish-black (N2)	Gritty, dense paste	Todorokite Smectite Quartz	Distinctly bedded	Infrequent penetion by worm tubes	Observed in a variety of combinations of layering with other sediment types; often in rather close association with both overlying dense manganese crust and underlying pale olive consolidated detrital sediment.
G	Altered detrital sediment	Dark yellowish-brown (10YR4/2)	Dense paste	Chlorite Smectite Illite Quartz Plagioclase	Distinctly bedded	Penetrated by worm tubes	Interlayered yellowish-brown, and brown, greasy-to-gritty, thick-to-thin-bedded, consolidated altered detrital sediment; most often appears just below the umberous lower manganese crust which caps the various layered combinations of hydrothermal and hydrothermally altered sediments, also capped frequently by layer F; frequently displays angular unconformities with overlying and underlying sediments; penetrated by very large (up to 1.5 cm diam.) worm tubes composed of agglutinated sediment.
H	--	--	--	Amorphous [$Fe(OH)_3$?]	----	----	Iron-oxide worm tube wall material - not classed as a sediment type.
I	Oxidized detrital sediment	Moderate yellowish-brown (10YR5/4) to dark yellowish-brown (10YR4/2)	Dense paste	Smectite Chlorite Illite Quartz Plagioclase	Thin, massive	Abundant to intense penetration by worm tubes	Caps, sometimes grades imperceptibly into pale olive detrital sediment, usually just below umberous lower manganese crust; most worm tubes are the iron-oxide type, some, as in the underlying pale olive ooze, are the nontronite-walled type.
J	Punky manganese deposit	Dusky yellowish-brown (10YR2/2)	Dense, crumby paste	Birnessite Natrobirnessite Todorokite Quartz	Thin, massive	Intense penetration by worm tubes	Thin layer just above I, layer probably admixed with the overlying umberous manganese crust which caps it; crowded with iron-based worm tubes.

Table 6. Chemical Analyses of Hydrothermal Nontronite/Mn-oxide Deposits Recovered in Dredge 16

Sample	Mn(%)	Fe(%)	Mo(ppm)	Zn(ppm)	Cu(ppm)	Ni(ppm)
1	0.14	28.75	<100	190	75	30
2	0.14	25.91	"	45	20	<30
3	0.16	18.39	"	120	45	70
4	0.14	17.94	"	75	35	55
5	0.15	15.27	"	110	50	65
6	5.80	14.31	200	130	60	70
7	21.95	7.62	330	115	45	65
8	37.09	2.13	385	170	85	175
9	43.19	1.14	1400	185	65	170
10	44.76	0.94	1700	110	250	975

Arranged in order of decreasing Fe. Pb and Co not detected at 50 ppm levels in any sample. Sample 1 corresponds to B, 2 to I, 3 to I, 4 to C, 5 to E, 6 to G, 7 to J, 8 to F, 9 to D, and 10 to A in Table 5. Samples similar but not identical to those analyzed by X-ray diffraction.

Analyst: R. Bouse; all analyses by atomic absorption spectrophotometry.

Table 7. Descriptions of marine oozes dredged from Gorda Ridge.

Dredge No.	Sample No.	Sediment Type	Color (wet)	Consolidation	Non-argillaceous constituents: Glass	Tests	Crystals	Manganese	Rock	Mineralogy (XRD)	Stratification	Bioturbation	Remarks
1	Sock	Ooze	Dark yellowish-brown (10YR4/2)	Pasty	Black (N1), vitrophyric (plagioclase/olivine)	Benthic foraminifers	None	None	None	Illite Chlorite Plagioclase Quartz Smectite	Bedded? (marbled)	Not detected	Abundant glass fragments related to Lithology 1 of lava descriptions; abundant benthic foraminifera.
2	Sock	Ooze	Light olive gray (5Y5/2)	Fluid to pasty	Black (N1), aphyric to porphyritic (plagioclase/olivine)	Benthic foraminifers	None	None	Basalt, medium dark gray (N4)	Illite Chlorite Smectite Plagioclase Quartz	Bedded? (marbled)	Not detected	Abundant glass fragments related to Lithologies 1 and 2 of lava descriptions; abundant benthic foraminifera.
3	9	Ooze	Olive gray (5Y4/1)	Pasty	Black (N1), porphyritic (plagioclase/olivine)	Benthic foraminifers	None	None	None	Illite Chlorite Smectite Plagioclase Quartz	Bedded? (marbled)	Not detected	Abundant benthic foraminifera; glass fragments related to Lithology 3 of lava descriptions; rock dredge sample.
	Sock	Ooze	Dark yellowish-brown (10YR4/2)	Fluid to pasty	Black (N1), porphyritic (plagioclase/olivine)	Benthic foraminifers	None	None	None	Illite Chlorite Smectite Plagioclase Quartz	Bedded? (marbled)	Not detected	Abundant benthic foraminifera; glass fragments related to Lithology 3 of lava descriptions; very small sample.
4	Sock	Ooze	Dark yellowish-brown (10YR4/2)	Fluid to pasty	Black (N1), Subaphyric (plagioclase/olivine)	Benthic foraminifers	None	None	Basalt, medium dark gray (N4)	Illite Chlorite Smectite Plagioclase Quartz	Unstratified	Not detected	Great abundance of benthic foraminifera; sample is mostly glass fragments related to Lithologies 1 and 2 of lava descriptions and protozoan tests - very small amount of sediment.
5				---- N O R E C O V E R Y ----									
6	Sock	Ooze	Dark yellowish-brown (10YR4/2)	Fluid to pasty	Black (N1), to grayish-black (N2), aphyric	Benthic foraminifers	None	None	Basalt, dark gray (N3) to medium dark gray (N4)	Illite Chlorite Smectite Plagioclase Quartz	Bedded? (marbled)	Not detected	Abundant glass fragments related to Lithologies 1 and 2 of lava descriptions; abundant benthic foraminifera.
7	1	Ooze	Dark olive gray (5Y3/1)	Pasty to lumpy	Black (N1), to grayish-ish black (N2), aphyric	Benthic foraminifers	Rare olivine	None	Basalt, dark gray (N3), small clay pellets, moderate reddish-brown (10R4/6) goethite(?) fragments	Illite Chlorite Smectite Plagioclase Quartz	Massive (lumpy part) to marbled (pasty part)	Small worm holes observed	Glass fragments related to Lithologies 1 and 3 of lava descriptions, benthic foraminifera; mud adhered to rock samples in rock dredge haul.
7	Sock	Ooze	Dark yellowish-brown (10YR3/2)	Pasty	None	None	None	None	None	Illite Chlorite Smectite Plagioclase Quartz	Bedded? (faintly marbled)	Not detected	No non-argillaceous components observed.
8				---- N O R E C O V E R Y ----									
9				---- N O S E D I M E N T S R E C O V E R E D ----									
10	Sock	Ooze	Dark yellowish-brown (10YR4/2)	Fluid to pasty	Black (N1), aphyric	Benthic foraminifers	Plagioclase, olivine	None	None	Illite Chlorite Smectite Plagioclase Quartz	Bedded? (marbled)	Not detected	Very small recovery consisting of ooze charged with basaltic glass fragments related to Lithology 1 of lava descriptions, crystal fragments, benthic foraminifera, and other minute tests and shells.
10	2	Ooze	Light olive gray (5Y5/2)	Pasty to compact lumpy	Black (N1), aphyric	Benthic foraminifers	None	None	None	Illite Chlorite Smectite Plagioclase Quartz	Bedded	Penetrated by worm tubes, holes	Small recovery, as above, consisting of flattish, rounded lumps of consolidated ooze displaying quite distinct and heterogeneous beds - some basalt glass-rich, some highly penetrated with worm tubes, set in pasty ooze; rock dredge sample.

Table 7. continued

Dredge No.	Sample No.	Sediment Type	Color (wet)	Consolidation	Non-argillaceous constituents: Glass	Tests	Crystals	Manganese	Rock	Mineralogy (XRD)	Stratification	Bioturbation	Remarks
11	Sock	Ooze with mudstone	Light olive gray (5Y4/2)	Pasty to lumpy	Black (N1), aphyric	Benthic foraminifers	None	None	None	Illite Chlorite Smectite Plagioclase Quartz	Bedded	Not detected	More stratified, consolidated than any previous material recovered: loose ooze set with basaltic glass fragments, related to Lithology 1 of lava descriptions; lumps of mudstone, and benthic foraminifera.
	2	Ooze	Light olive gray (5Y4/2)	Pasty to lumpy	Black (N1), aphyric	Benthic foraminifers	None	Micronodules	None	Illite Chlorite Smectite Plagioclase Quartz	Bedded	Not detected	Voluminous ooze with clay lumps filling cavity in large pillow basalt blister; rock dredge sample.
	7	Ooze/hydrothermal clay(?)	Olive hues: (10Y7/4) (10Y6/2) (5Y5/2)	Compact to crumby	None	None	None	None	None	Illite Nontronite Chlorite Smectite Plagioclase Quartz	Bedded	Burrowed	Varicolored baked ooze(?) or hydrothermal clay found in broken flat vesicles or drainout cavities in pillow basalt fragment; found in distinct layers covering thin coatings of vernadite(?)/hematite(?): moderate greenish-yellow (10Y7/4); pale olive green (10Y6/2), light olive gray (5Y5/2); rock dredge sample.
12	Sock	Ooze	Dark yellowish-brown (10YR3/2)	Pasty to fluid	Black (N1), aphyric	Benthic foraminifers	None	None	Basalt, dark gray (N3), aphyric	Illite Chlorite Smectite Plagioclase Quartz	Bedded? (marbled)	Not detected	Rare, generally small benthic foraminifera, basaltic glass fragments related to Lithology 1 of lava descriptions, rare basalt fragments.
13	Sock	Ooze	Dark yellowish-brown (10YR4/2)	Fluid to pasty	Black (N1), aphyric	Benthic foraminifers	None	None	None	Illite Chlorite Smectite Plagioclase Quartz	Bedded? (marbled)	Not detected	Rare benthic foraminifera, abundant basaltic glass fragments probably related to Lithology 1 of lava descriptions, some up to 3 cm in diameter (some original glass surfaces, striated, developed palagonitization), glass septae.
14	Sock	Ooze	Dusky yellowish-brown (10YR2/2)	Fluid to pasty	Black (N1), aphyric	Benthic foraminifers	None	None	None	Illite Chlorite Smectite Plagioclase Quartz	Bedded? (marbled)	Not detected	Very rare benthic foraminifera, abundant basaltic glass fragments up to 2 cm in diameter probably related to Lithology 1 of lava descriptions (one remnant original glass surface(?) coated thinly with hematite(?), incipient palagonitization), most are conchoidally-fractured fragments
15	2	Ooze	Olive gray (5Y4/1)	Pasty	Black (N1), subaphyric		None	None	Basalt, dark gray (N3), subaphyric (olivine)	Illite Chlorite Smectite Plagioclase Quartz	Bedded? (marbled)	Not detected	Rare benthic foraminifera, basaltic glass and rock fragments related to Lithology 1 of lava descriptions; rock dredge sample.
	Sock	Ooze	Olive gray (5Y4/1) to dark yellowish-brown (10YR4/2)	Pasty to fluid	Black (N1), subaphyric (olivine)	Benthic foraminifers	None	None	Clay pellets, basalt, dark gray (N3) subaphyric (olivine), siltstone(?)	Illite Chlorite Smectite Plagioclase Quartz	Bedded? (marbled)	Not detected	Sock dredge sample divided into two different-colored oozes with slightly different compositions: top of sock is olive gray ooze with abundant small clay pellets (probably of same composition) and scarcity of tests, glass, rock fragments; bottom of sock is dark yellowish-brown ooze, with much greater abundance of clay pellets, lumps, siltstone(?) fragments, tests, glass, and rock fragments related to Lithology 1 of lava descriptions.
16	Sock	Ooze	Dusky yellowish-brown (10YR2/2)	Fluid to pasty, lumpy	Black (N1), porphyritic (plagioclase/olivine)	Benthic foraminifers	Plagioclase, olivine	Fragmented crust from pillow rind	None	Illite Chlorite Smectite Plagioclase Quartz Goethite? Vernadite?	Bedded? (marbled)	Not detected	Rare benthic foraminifera, fragments of glassy basaltic pillow rind related to Lithology 1 of lava descriptions, abundant metal oxide-rich ooze in varying states of consolidation.
17	17	Ooze	Light olive gray (5Y5/2)	Thin to thick paste	None	None	None	Crust fragments, dusky yellowish-brown (10YR2/2)	Clay pellets	Illite Chlorite Smectite Plagioclase Quartz	Bedded? (faintly marbled)	Not detected	Rather barren, homogeneous ooze containing a few fragments of manganese crusts and a few pellets; rock dredge sample.
	Sock	Ooze	Dark yellowish-brown (10YR4/2)	Thin to thick paste	Black (N1), aphyric	Planktonic, benthic foraminifers	Plagioclase, olivine	Crust fragments, as above	Clay pellets, siltstone(?), basalt fragments	Illite Chlorite Smectite Plagioclase Quartz	Bedded? (marbled)	Not detected	Mostly foraminiferal tests (primarily planktonic) held loosely together with clay ooze; also includes smaller amounts of clay pellets, siltstone(?); basalt, and basaltic glass fragments related to Lithology 1 of lava descriptions.

Table 8. Gorda Ridge - Clay Mineralogy of Sediments

Sample No.	%Smectite	%Illite	%Chlorite
D1 SOCK	21	33	46
D2 SOCK	22	32	46
D3 SOCK	24	30	46
D3 MUD	21	32	47
D4 SOCK	19	32	49
D6 SOCK	24	28	48
D7 SOCK	27	27	46
D7 MUD	56	19	25
D10 SOCK	25	26	49
D11 SOCK	33	28	39
D11 MUD	23	30	47
D12 SOCK	26	28	46
D13 SOCK	30	28	42
D14 SOCK	32	26	42
D15 TOP OF SOCK	34	27	39
D15 BOTTOM OF SOCK	21	35	44
D16 SOCK	25	32	43
D17 SOCK	37	26	37
D17 MUD	35	27	38

All samples have 6.2°2θ chlorite peak about 50% that of the 12.5°2θ chlorite peak. Sample preparation: 10cc of <63μm fraction was soaked for >2 days in water; Morgan's solution (Na-acetate + glacial acetic acid in water); and 30% hydrogen peroxide in a 5:2:2 ratio. Samples were then washed in Morgan's solution, treated with 2% sodium carbonate, and washed with a 0.01% sodium carbonate solution. The clays (<2μ) were suspended in a low speed (850 rpm) centrifuge, decanted and collected; saturated with 1 m magnesium chloride, x-rayed, saturated in ethylene glycol, and x-rayed again.

Table 9. Gorda Ridge - Composition of Sediments

Gray Muds	Mn	Fe	Zn	Ni	Cu	Co	Pb	Mo
D7 MUD	.21%	5.67%	210ppm	210ppm	120ppm	<50ppm	270ppm	<100ppm
D3 MUD	.08%	5.44%	220	185	95	"	<50ppm	"
D11 SOCK	.12%	5.28%	225	180	100	"	"	"
D17 MUD	.07%	6.40%	190	170	60	"	"	"
D2 SOCK	.15%	5.52%	215	175	90	"	"	"
D15 TOP OF SOCK)	.29%	5.39%	200	155	105	"	"	"
Light Brown Muds								
D6 SOCK	.25%	5.81%	185	170	90	"	"	"
D3 SOCK	.27%	5.57%	215	180	90	"	"	"
D10 SOCK	.43%	5.47%	200	190	105	"	"	"
Dark Brown Mud								
D7 SOCK	.36%	5.64%	200	190	105	"	"	"
Choc. Brown muds								
D1 SOCK	.53%	5.70%	275	200	100	"	"	"
D15 BOTTOM OF SOCK	.41%	5.24%	150	145	80	"	"	"
D12 SOCK	1.16%	5.56%	210	200	105	"	"	"
D16 SOCK	1.43%	5.43%	170	155	95	"	"	"

Analyst: Robin Bouse; all analyses by atomic absorption spectrophotometry. Samples arranged in increasing color intensity from top to bottom.

TABLE 10. List of Foraminifers

AGGLUTINATED BENTHIC

Adercotryma glomeratum

A. sp.
Ammobaculites
Ammodiscus spp.
Ammolagena
Ammomarginulina
Astrorhiza

Bathysiphon
Bottlelina

Cribrostomoides
Cyclammina
Cystammina

Eggerella

Glomospira
Globotextularia anceps

Haplophragmoides columbiense
H. sp.
Hemisphaerammina
Hormosina globulifera
Hyperammina elongata

Karreriella

Lituotuba

Martinottiella

Protobotellina
Psammosphaera fusca
P. parva

Recurvoides contortus
R. sp.
Reophax difflugiformis
R. distans
R. guttifer
R. nodulosus
Reophax sp.
Rhabdammina abyssorum
R. irregularis
R. spp.
Rhizammina algaeformis

Saccammina
Saccorhiza ramosa
Spiroplectammina spp.

Textularia
Thurammina
Tolypammina
Trochammina spp.
Trochamminoides
Unidentifiable to genus:
Family Saccamminidae
Subfamily Diffusilininae (See Loeblich and Tappan, 1964)
(This form has a clayey exterior with complex or honeycomb interior).

TABLE 10 (Cont'd)

CALCAREOUS BENTHIC

Bolivina
Bulimina spp.
Buliminella tenuata

Cassidulina spp.
Chilostomella
Chilostomellina
Cibicides
Cibicidina
Cibicidoides

Dentalina

Ehrenbergina
Epistominella
Eponides leviculus
E. tener
E. spp.

Fissurina
Fursenkoina

Globobulimina spp.
Gyroidina

Hoeglundina

Lagena
Laticarinina

Marginulina
Melonis
miliollids(undifferentiated)

Nodosaria

Planispirinoides bucculenta
Pullenia spp.
Pyrgo
Pyrgoella

Sphaerodina

Triloculina

Uvigerina spp.

Valvulineria

PLANKTONIC FORAMINIFERS
Globigerina
Orbulina

TABLE 11. Summary of foraminiferal fauna characteristics.

Sample no.	Specimen abundance benthic	Specimen abundance plantonic	Test Size (>1.0mm)	Test composition	Volc. glass	Species diversity	Preservation
D1 SOCK	A	R	Y	aggl.>>calc.	+	H	G
D2 SOCK	A	R	Y	aggl.>>calc.	++	H	G
D3 SOCK	A	R	Y	aggl.>>calc.	+	H	G
D3 MUD	A	C	N	calc.>aggl.	-	H	G
D4 SOCK	A	X	Y	aggl.>>calc.	++	H	G
D6 SOCK	A	R	Y	aggl.>>calc.	+	H	G-
D6 MUD	R	X	N	all aggl.	-	M	M+
D7 SOCK	R	R	Y-	aggl.>>calc.	-	M	M
D7 MUD	R	X	N	one aggl.	0	L	X
D10 SOCK	C	C	Y	aggl.>>calc.	-	M	M-
D11 SOCK	C	C	N	calc.>>aggl.	-	M	G
D12 SOCK	A	C	Y	aggl.>>calc.	-	H	M-
D13 SOCK	R	X	N	aggl.>>calc.	-	M	M
D14 SOCK	R	X	N	aggl.>>calc.	-	H-	M
D15 TOP OF SOCK	C	C	Y	aggl.>>calc.	-	M	M
D15 BOTTOM OF SOCK	A	C	Y+	aggl.>>calc.	+	M+	M-
D16 SOCK	A	C-	Y+	aggl.>>calc.	+	H	M
D17 SOCK	A	A	Y+	aggl.=calc.	0	H	M-
D17 MUD	C	A	N	calc.>>aggl.	0	M-	G-

Explanation: Specimen abundance; A(abundant)=>500 individuals, C(common)=<500>100, R(Rare)=<100>1, X=absent
Test size: (Presence of large>1.0mm agglutinated forms); Y-Yes; N=No
Test Composition: aggl.=agglutinated foraminifers; calc.=calcareous foraminifers; ++=much volcanic glass used in test construction; -=less use of volcanic glass; 0=volcanic glass not used;
Species diversity: H(High)=>20 species; M(Moderate)=<20>10 species; L(Low)=<10species
Preservation: G(Good)=Little iron stain; most specimens not broken; M(Moderate)=M+=more stain; more broken specimens
M-=most stain; most broken specimens

TABLE 12. Summary of diatom, radiolarian, silicoflagellate, and coccolith abundance.

Sample no.	Diatoms	Radiolarians (smear slides) <0.063mm	Radiolarians* (>0.063mm)	Silicoflagellates	Coccoliths
D1 SOCK	R	X	A	R	X
D2 SOCK	C	X	A	C	X
D3 SOCK	C	R	A	C	R
D3 MUD	C	C	A+	R	R
D4 SOCK	R	R	R	R	X
D6 SOCK	C	X	R	R	X
D6 MUD	C	C	A	R	X
D7 SOCK	C	X	A	C	X
D7 MUD	A	R	R	R	X
D10 SOCK	C	C	C+	R	R
D11 SOCK	C	A	A	A	C
D12 SOCK	R	R	A	C	X
D13 SOCK	R	R	C	R	X
D14 SOCK	R	C	R	R	X
D15 TOP OF SOCK	C	R	C	C	C
D15 BOTTOM OF SOCK	R	C	C	R	R
D16 SOCK	R	R	C	R	C
D17 SOCK	R	R	R	X	A
D17 MUD	X	X	X	X	X

Explanation of symbols

Diatoms	Radiolarians (smear slides) <.063mm	Radiolarians* (>.063mm) visual estimate	Silicoflagellates	Coccoliths
A≥100	A≥15		A≥20	A≥400
C<100≥50	C<15≥8		C<20≥10	C<400≥20
R<50≥1	R<8≥1		R<10≥2	R<20≥1
X = absent	X = absent		X = absent	X = absent

See text for details of analysis.

FIGURE AND PLATE CAPTIONS

Figure 1. Regional location map showing the Gorda, Juan de Fuca and Explorer Ridge spreading centers off the Pacific northwest. The Gorda Ridge is bounded to the north by the Blanco Transform and the south by the Mendocino Fracture Zone. The southern third of the Gorda Ridge is a sediment filled trough named the Escanaba Trough. Known locations of massive hydrothermal sulfide deposits and of hydrothermal nontronite deposits are identified by different symbols.

Figure 2. Trackline chart for U.S.G.S. cruises L11-83-NC, L12-80-WF and KK2-83-NP are shown with dredge locations for 17 dredges stations during cruise KK2-83-NP. Previous dredge locations are shown as solid squares (Kay et al., 1970; Wakeham, 1978; Melson et al., 1977). Tracklines for two multichannel seismic reflection profiles across the Escanaba Trough shown as Figures 5 and 6 are indicated as lines 114 and 118.

Figure 3. Track chart of R/V Kana Keoki cruise KK1-83-NP. This chart shows the area covered by the vessel during the period from 26 September to 6 October 1983. A variety of geophysical data were collected during this cruise, including: 1) SeaMARC II side-scan sonar, 2) single channel seismic reflection, 3) gravity, 4) magnetics, and 5) 3.5 kHz bathymetry. The trackline numbers are keyed to seismic reflection records shown in Figure 4. The letters B and G indicate crossings of the Blanco Fracture Zone and Gorda Ridge axial graben, respectively. The numbered boxes indicate the location of specific examples of the SeaMARC II imagery shown in Figure 7.

Figure 4. Single-channel air gun seismic reflection records across Gorda Ridge. Line numbers shown on the individual record sections are keyed to trackline number in figure 3. The seismic records were collected along NW-SE tracks and have been "rotated" approximately 45° to align them for this figure. This process produces some spatial distortion because of the differences in horizontal and vertical scales of the seismic records (vertical exaggeration = 13:1). The letters B and G on the records refer to crossings of the Blanco Fracture Zone and Gorda Ridge axial valley, respectively.

Figure 5. Preliminary brute stack of line 114 over the Escanaba Trough near 41°N. Where it can be identified, the sediment-basement contact is indicated. Several small faults whithin the axial valley are also indicated. Note that east is the left on this plot.

Figure 6. Preliminary brute stack of line 118 over the Escanaba Trough near 40°30'N. The sediment-basement contact can be identified near the two ends of the profile. Beneath the ridge axis, the queried line indicates the approximate location of the contact.

Figure 7. Examples of SeaMARC II side-scan sonar imagery over Gorda Ridge. Preliminary processing (corrections for slant range and ship speed) was done in real time on board R/V Kana Keoki. The locations of each of the three images are shown on the trackline chart in Figure 3. Vessel speed was approximately 7.5 knots. The images are generated by sound pulses travelling from the center (white stripe) of the image outward. The effect is similar to an aerial photograph in which the ground is being illuminated by a "sun" at the center of the image. These images are optically "reversed", in that strong signals are shown as dark area; weak signals or shadow zones show as light areas.

Plate 1. Scanning electron micrographs of sulfides in lavas from dredge 7.
- A. Unaltered hexagonal plates of pyrrhotite on smectite. Material in upper right hand corner is manganosiderite (a Fe, Mn, Ca - carbonate).
- B. Corroded hexagonal plates of pyrrhotite on smectite.
- C. Enlargement of manganosiderite shown in A.
- D. Rounded pyrite cubes on smectite.
- E. Corroded pyrite in smectite.
- F. Euhedral barite crystals projecting into open cavity.
- G. Euhedral pyrite crystal projecting into open cavity.
- H. Euhedral barite (left), corroded sphalerite (center) and euhedral and corroded pyrite (right center, right edge).
- I. Enlargement of euhedral barite in H. Note small pyrite crystals on the smectite.

Plate 2. Scanning electron micrographs of agglutinated foraminifers.
1. Rhabdammina? sp. View looking down tube to show complex interior.
2. Astrorhiza sp.
3. Psammosphaera parva?. Note the blade-like piece of volcanic glass.
4. Rhabdammina abyssorum

Plate 3. Scanning electron micrographs of agglutinated foraminifers.
1-5. Reophax spp. Note large pieces of volcanic glass.

Plate 4. Scanning electron micrographs of agglutinated foraminifers.
1 and 2. Coiled agglutinated benthic foraminifers. Note large fragments of volcanic glass.
3. Ammodiscus sp.
4. Bathysiphon sp.

FIGURE 1

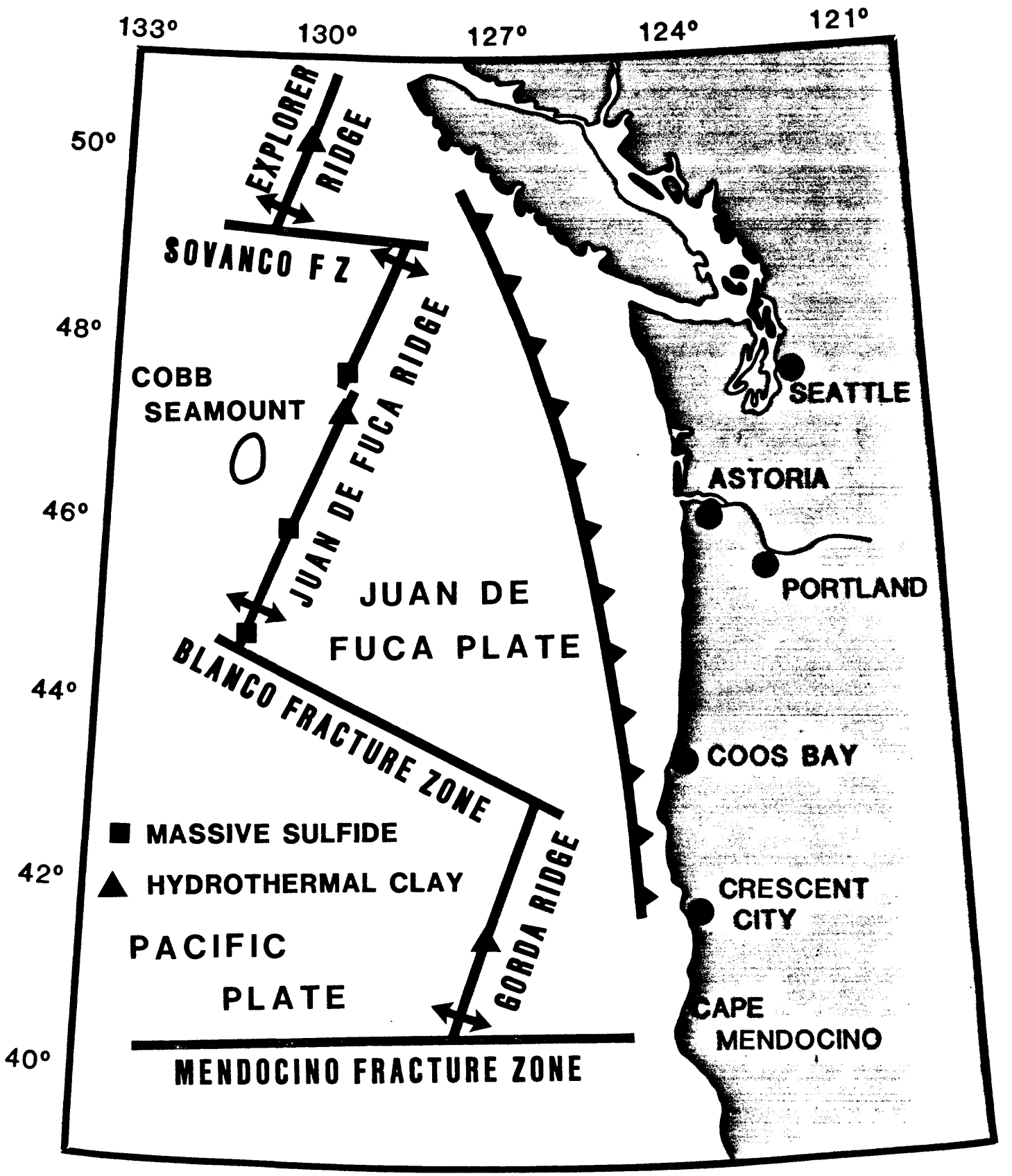
133°
130°
127°
124°
121°
50°
48°
46°
44°
42°
40°
EXPLORER RIDGE
SOVANCO FZ
COBB SEAMOUNT
JUAN DE FUCA RIDGE
JUAN DE FUCA PLATE
BLANCO FRACTURE ZONE
GORDA RIDGE
MASSIVE SULFIDE
HYDROTHERMAL CLAY
PACIFIC PLATE
MENDOCINO FRACTURE ZONE
SEATTLE
ASTORIA
PORTLAND
COOS BAY
CRESCENT CITY
CAPE MENDOCINO

FIGURE 2

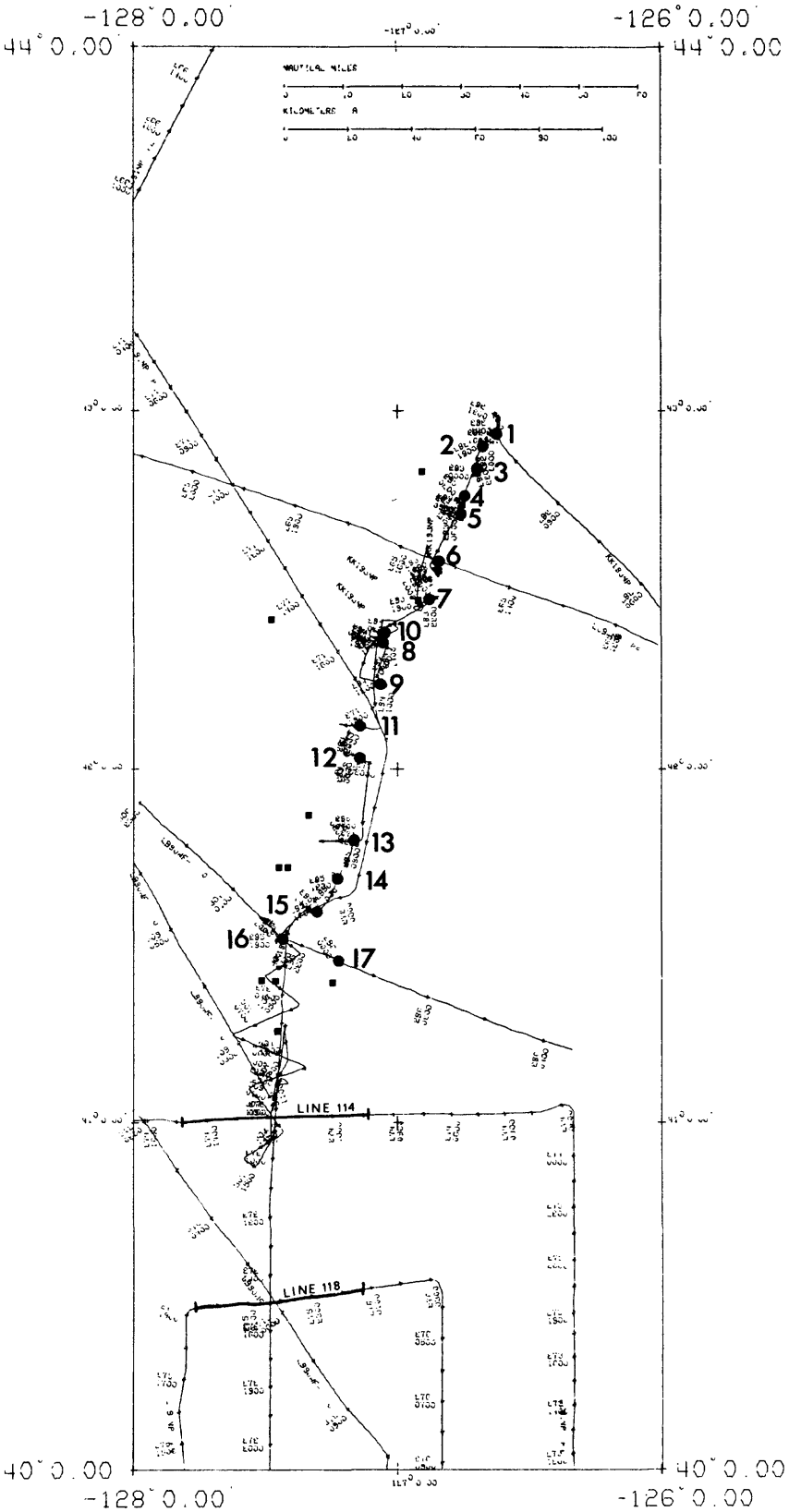
-128° 0.00
-126° 0.00
44° 0.00
40° 0.00
1
2
3
4
5
6
7
8
9
10
11
12
13
14
15
16
17
LINE 114
LINE 118

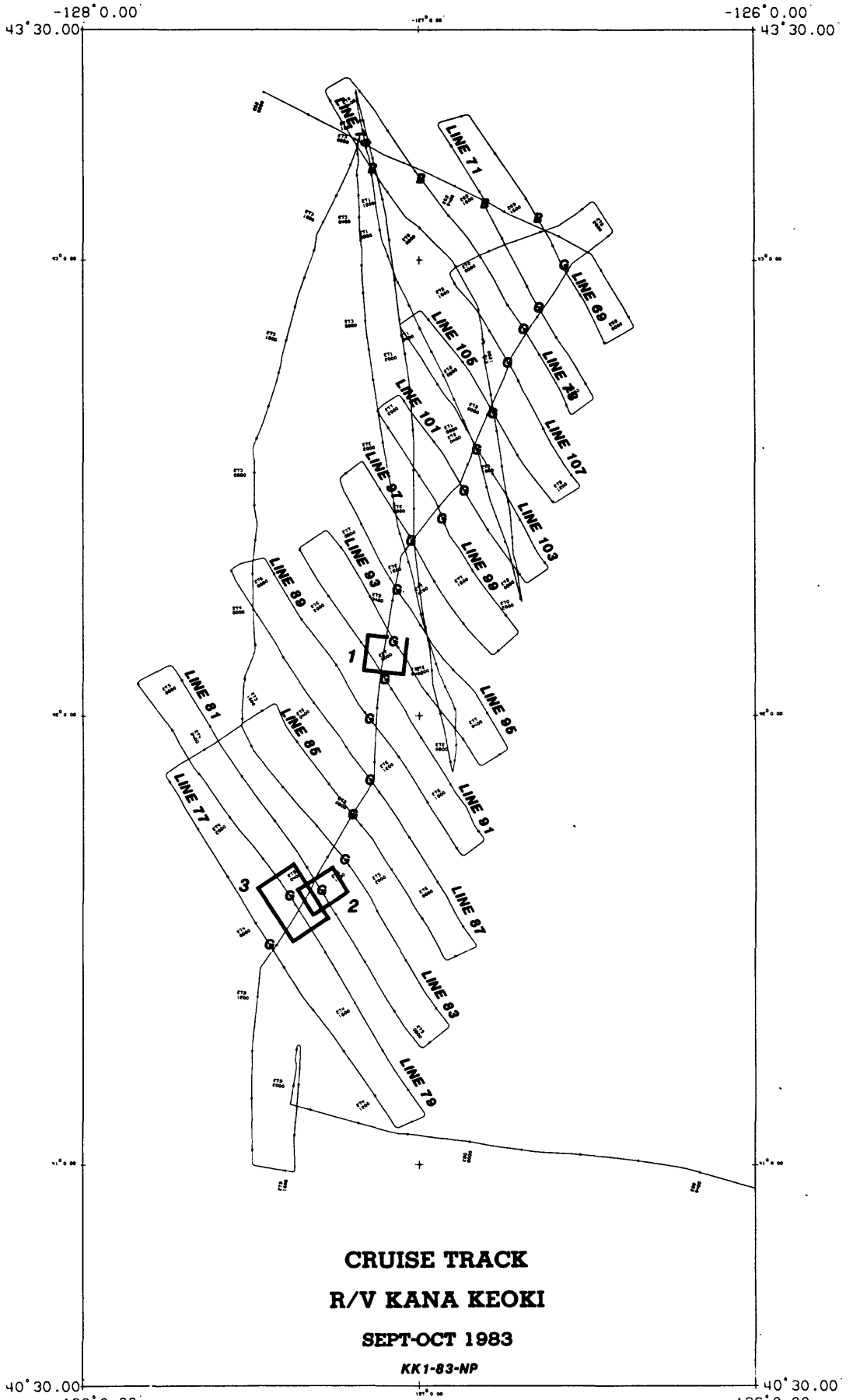

CRUISE TRACK

R/V KANA KEOKI

SEPT-OCT 1983

KK1-83-NP

FIGURE 3

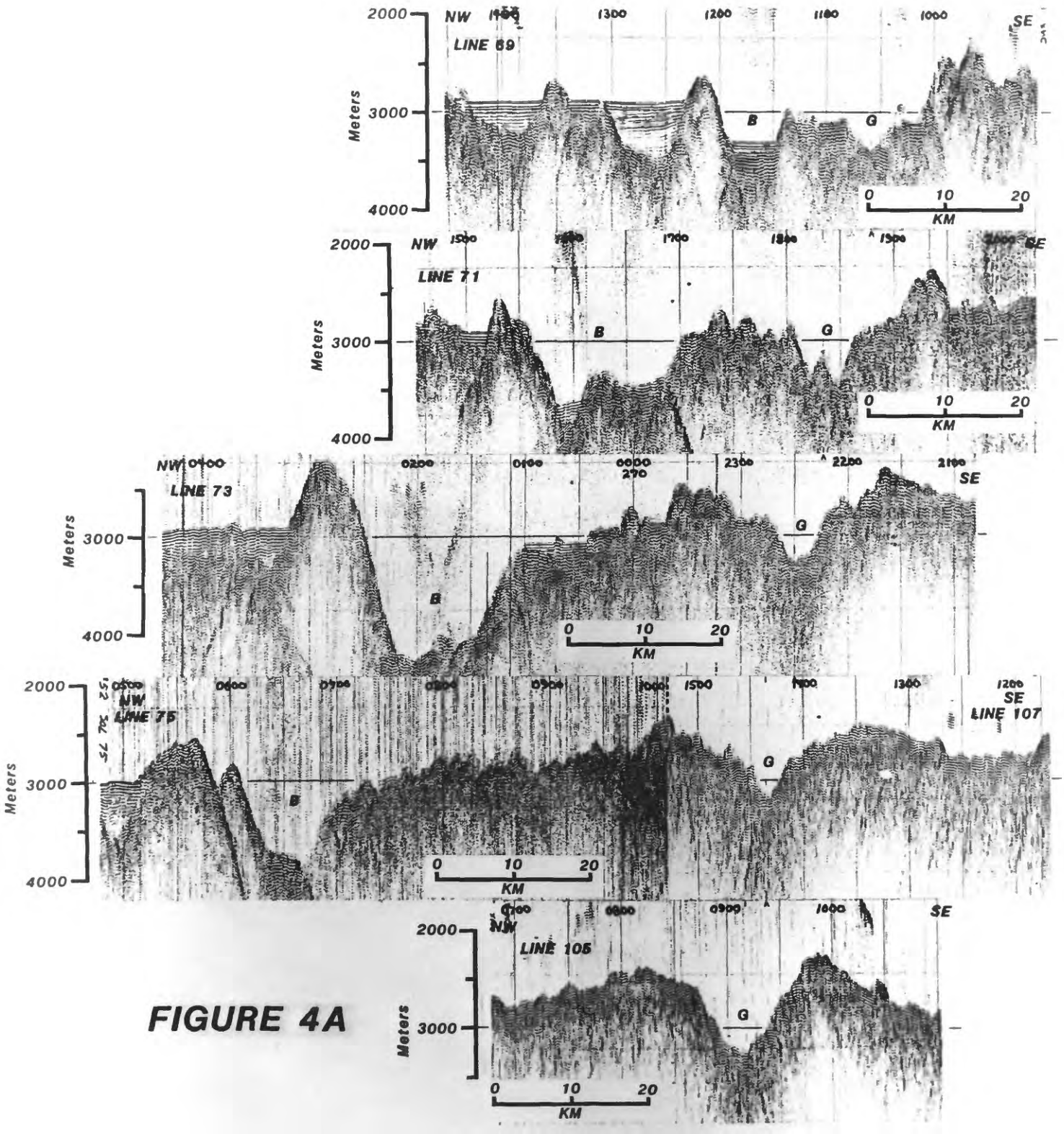
LINE 69
NW
SE
1300
1200
1100
1000
2000
3000
4000
Meters
B
G
0 10 20
KM
LINE 71
NW
SE
1500
1700
1800
1900
2000
3000
4000
Meters
B
G
0 10 20
KM
LINE 73
NW
SE
0400
0200
0100
0000
270
2300
2200
2100
3000
4000
Meters
B
G
0 10 20
KM
LINE 75
NW
SE
LINE 107
0500
0600
0700
0800
0900
1000
1500
1400
1300
1200
2000
3000
4000
Meters
B
G
0 10 20
KM
LINE 105
NW
SE
0800
0900
1000
2000
3000
Meters
G
0 10 20
KM

FIGURE 4A

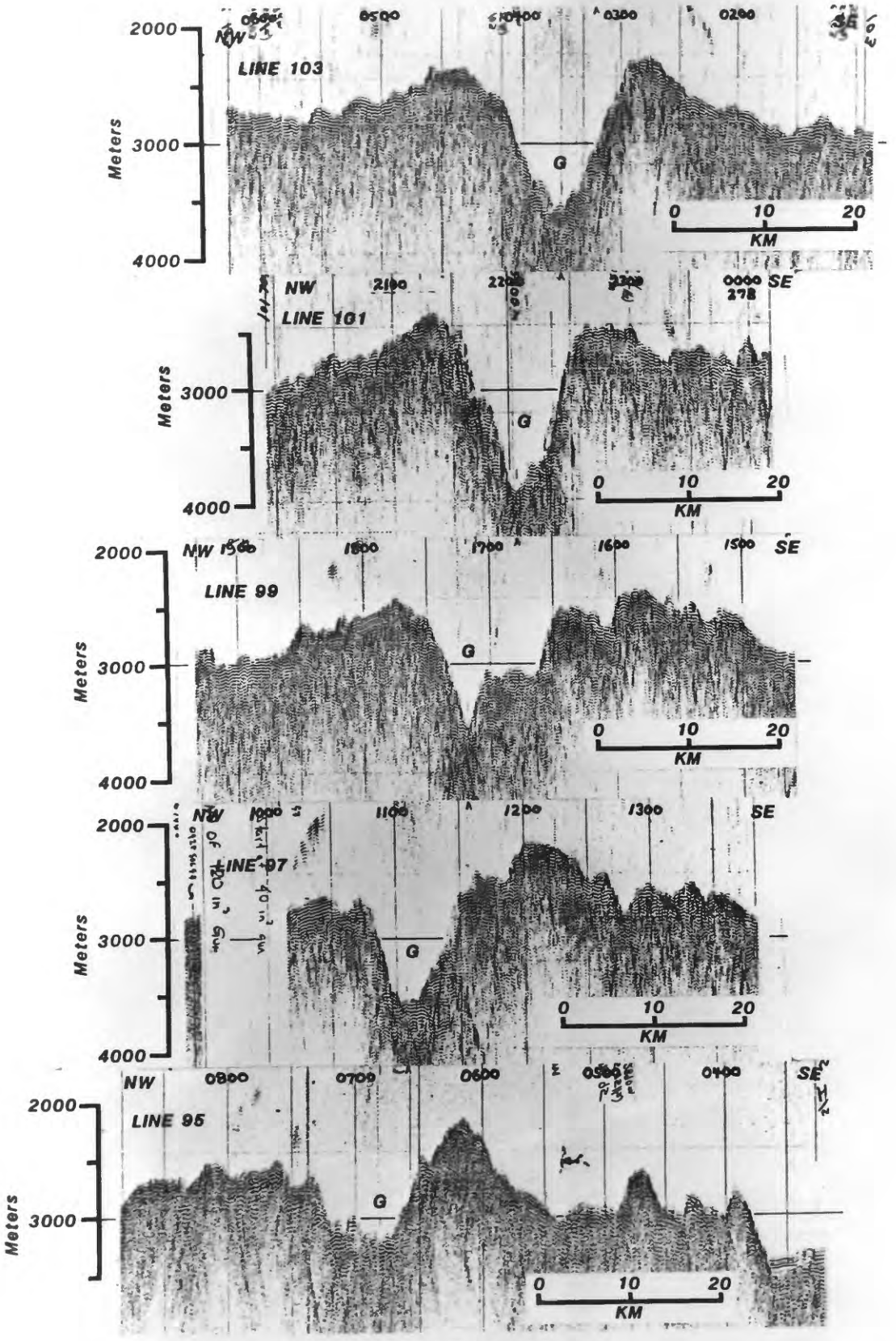
LINE 103
NW
SE
Meters
2000
3000
4000
G
0 10 20
KM
LINE 101
LINE 99
LINE 97
LINE 95

FIGURE 4B

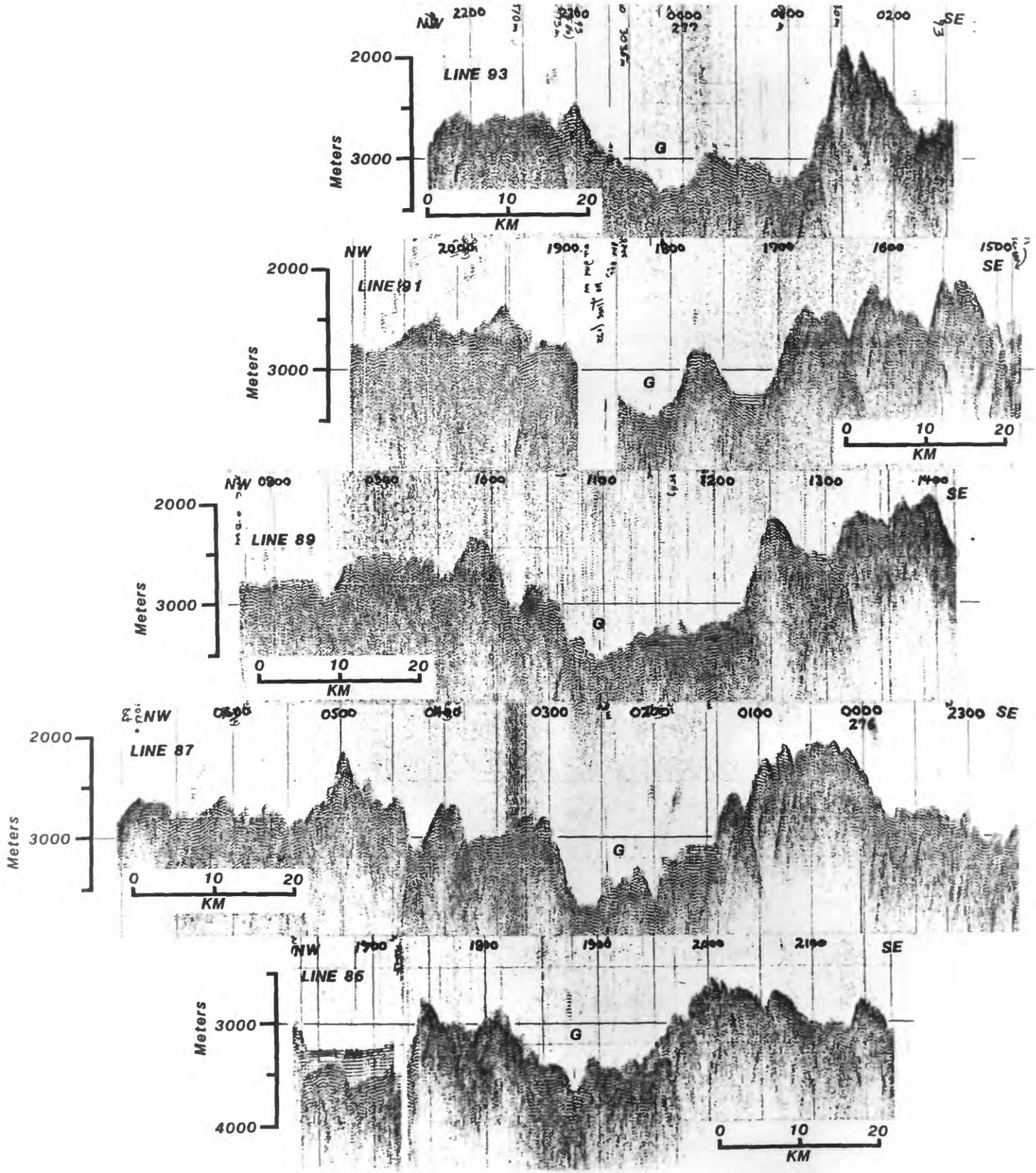
NW
SE
LINE 93
LINE 91
LINE 89
LINE 87
LINE 86
Meters
2000
3000
4000
G
0
10
20
KM

FIGURE 4C

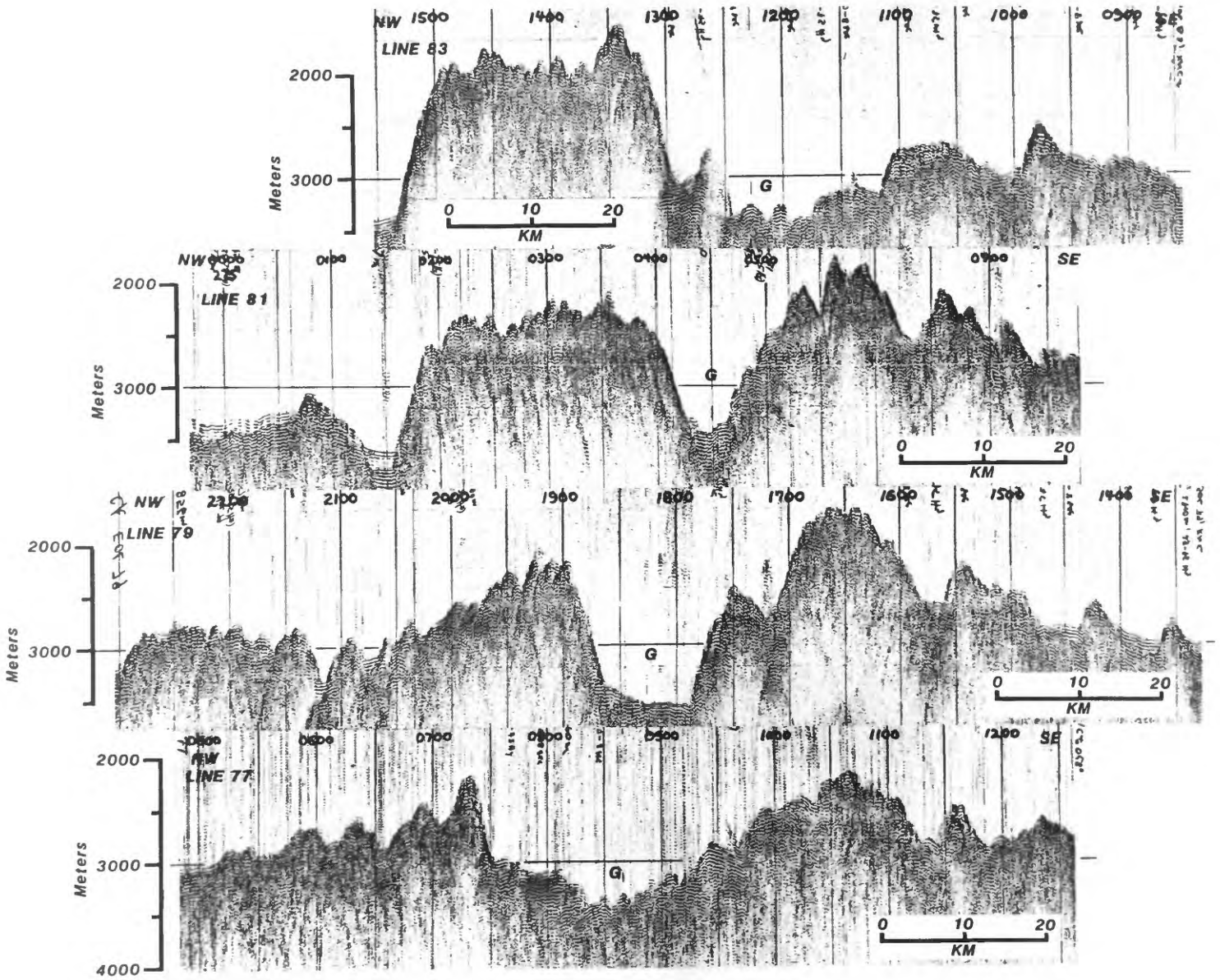
NW 1500
1400
1300
1200
1100
1000
0900
SE
LINE 83
2000
3000
Meters
G
0 10 20
KM
NW
0200
0300
0400
0500
0600
0700
SE
LINE 81
2000
3000
Meters
G
0 10 20
KM
NW
2200
2100
2000
1900
1800
1700
1600
1500
1400
SE
LINE 79
2000
3000
Meters
G
0 10 20
KM
0600
0700
0800
0900
1000
1100
1200
SE
NW
LINE 77
2000
3000
4000
Meters
G
0 10 20
KM

FIGURE 4D

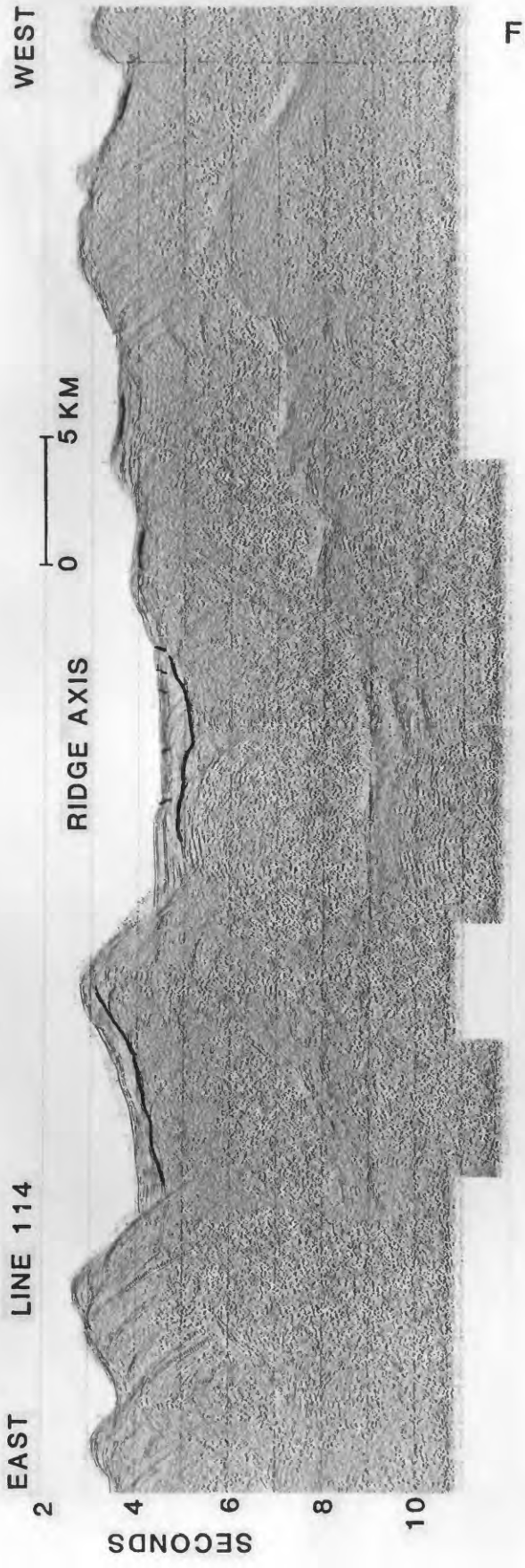

FIGURE 5

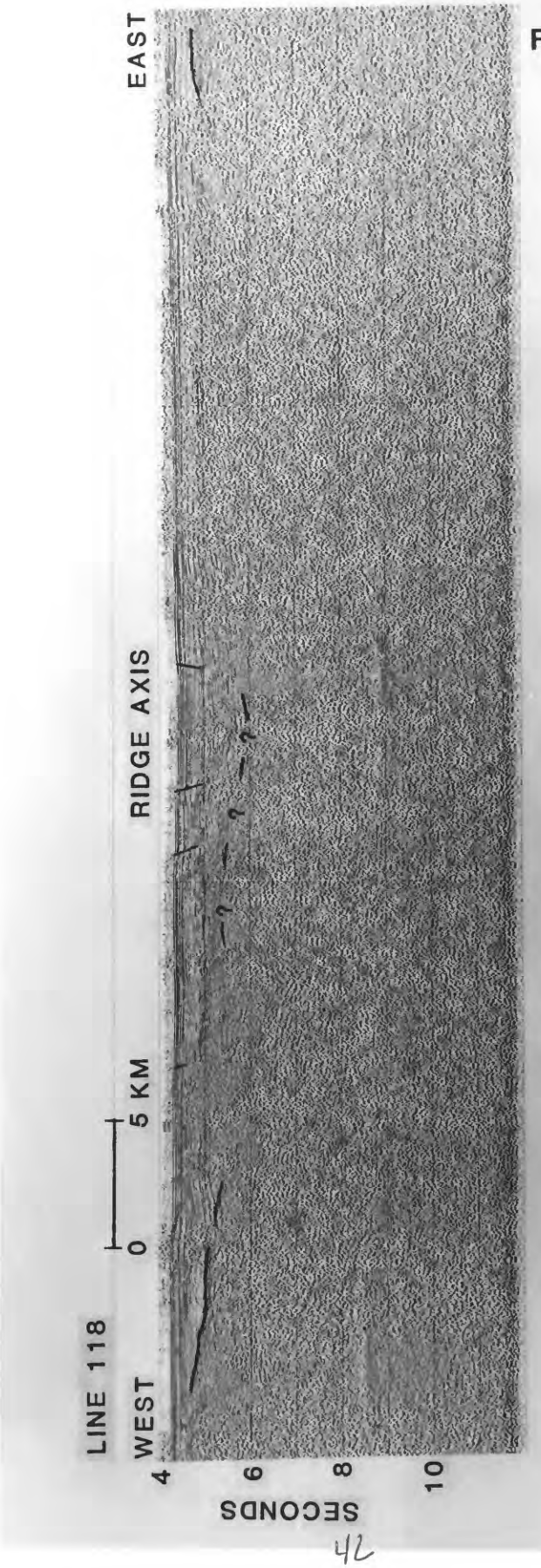

FIGURE 6

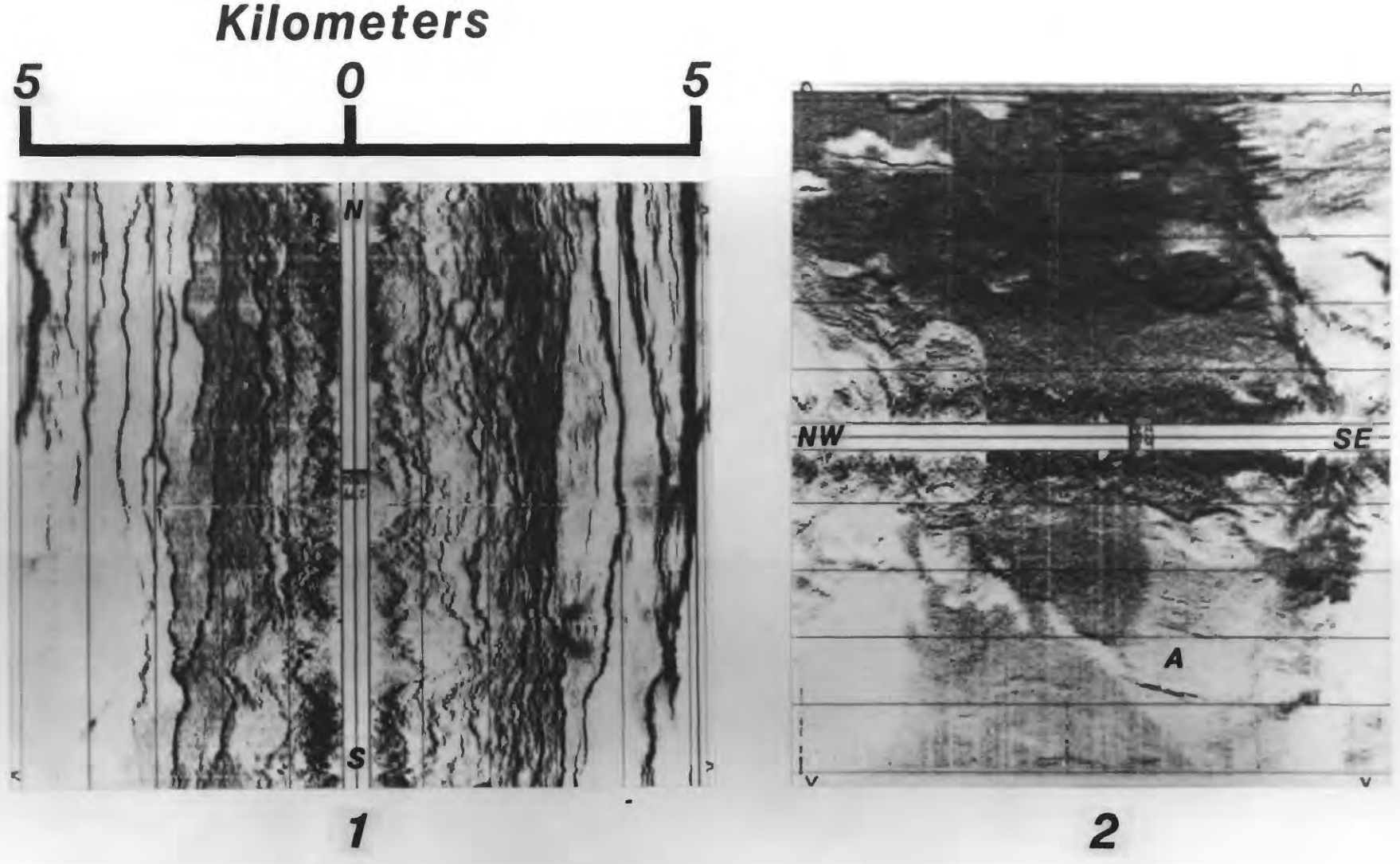

FIGURE 7

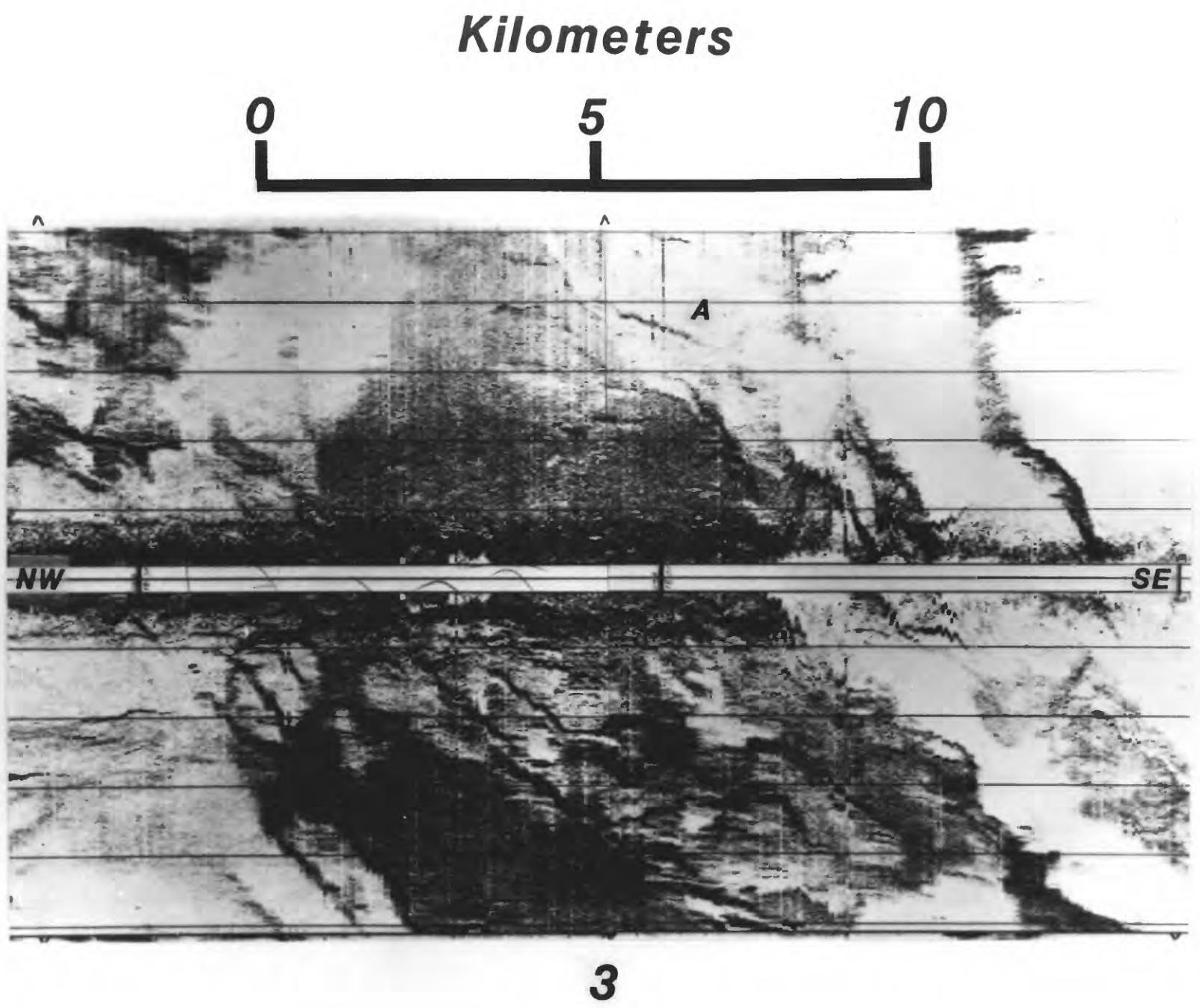

FIGURE 7

PLATE 1A-1F

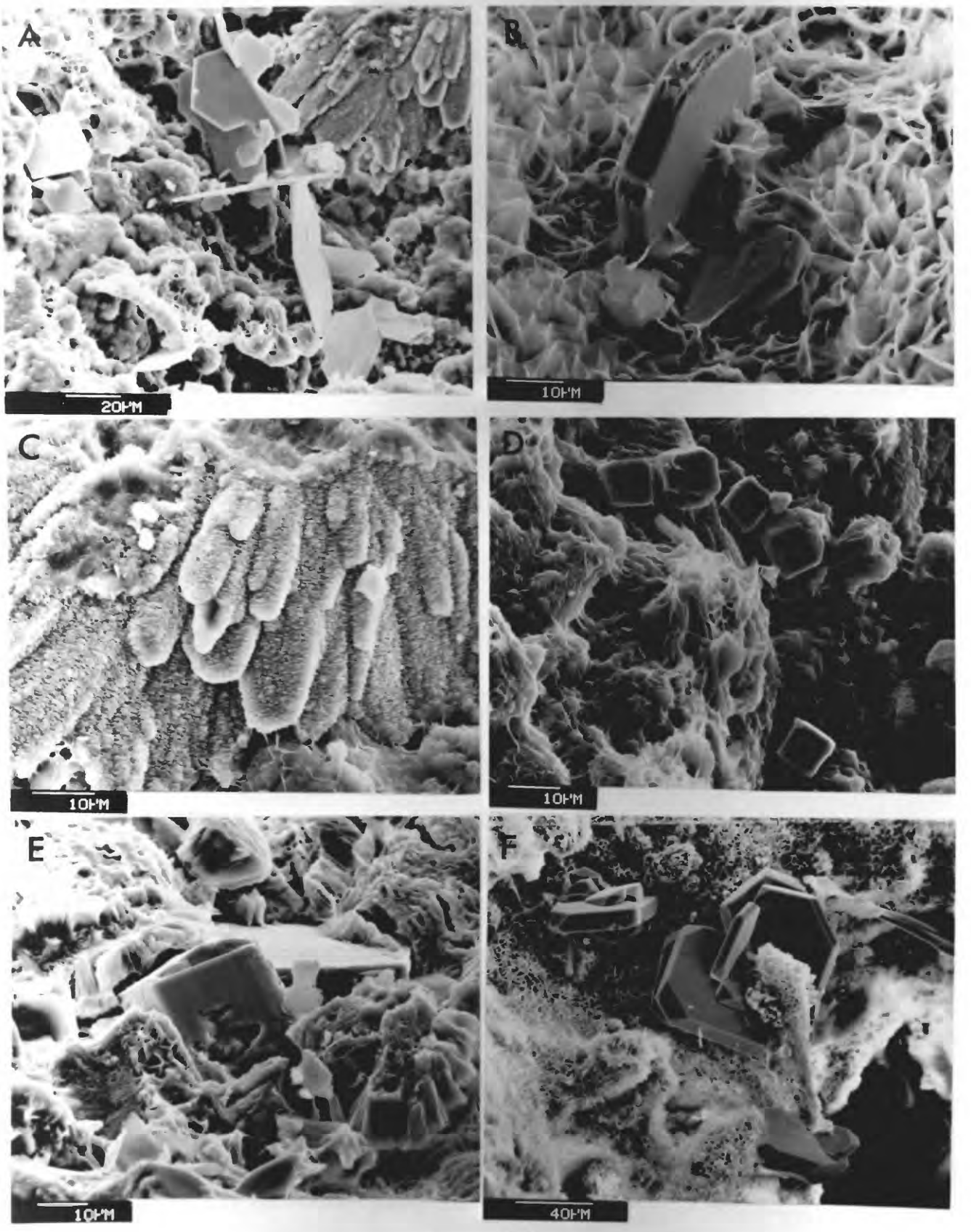

PLATE 1G-1I

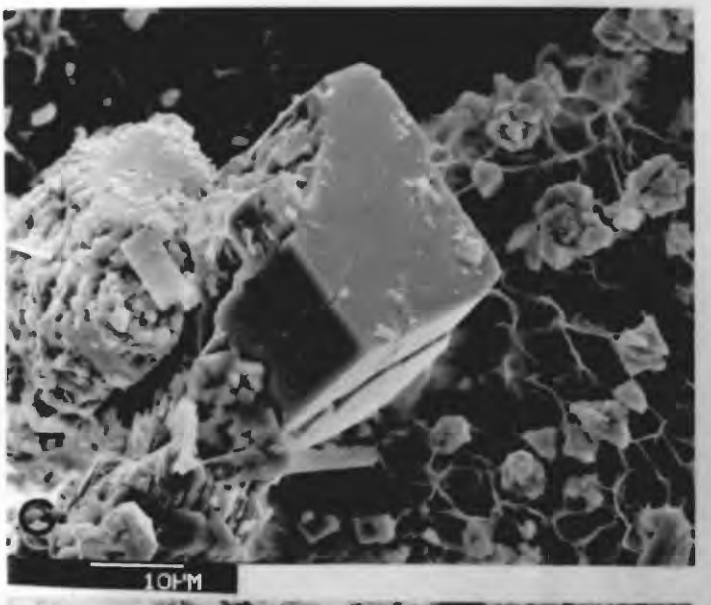

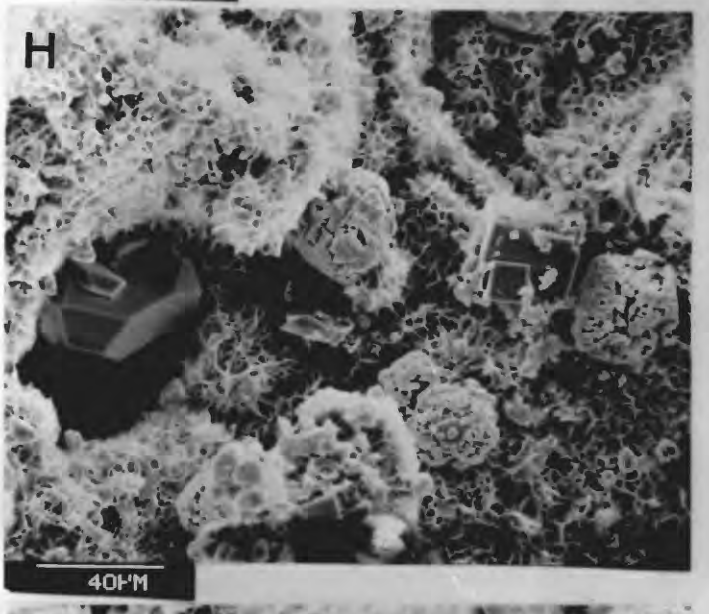

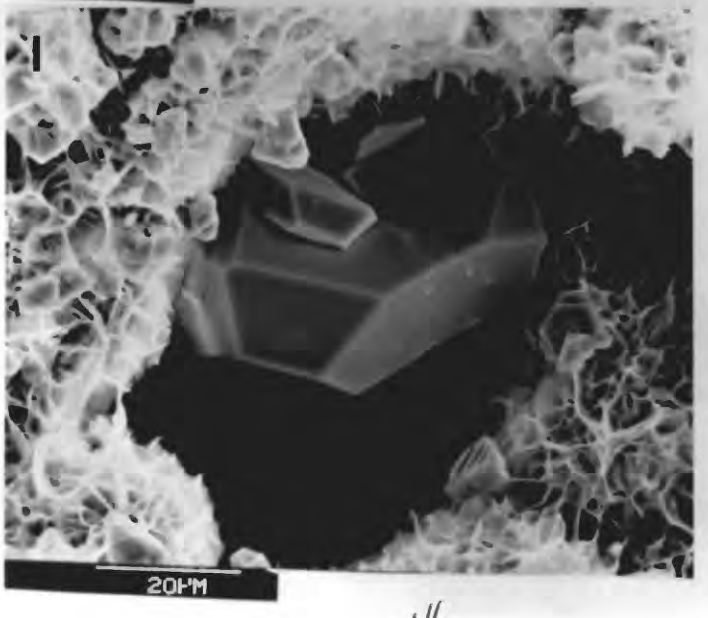

PLATE 2

1

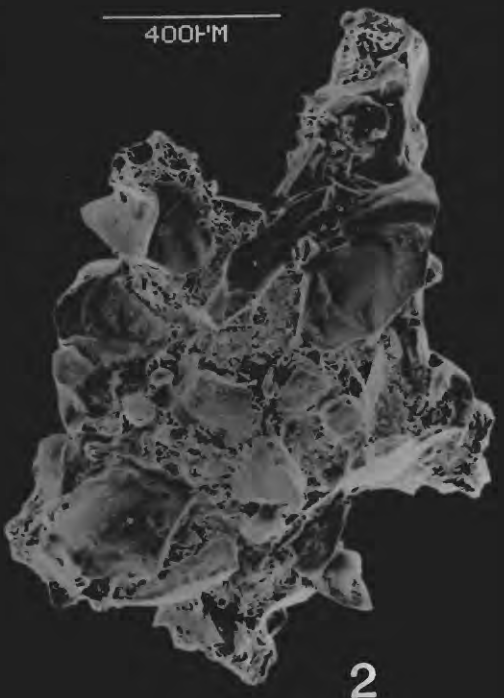

2

3

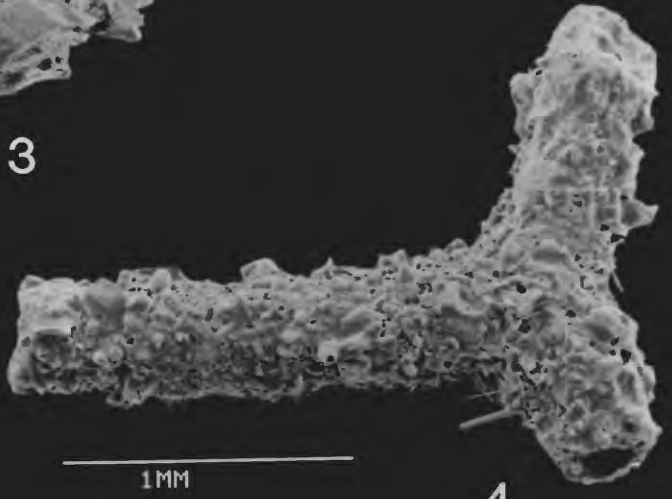

4

PLATE 3

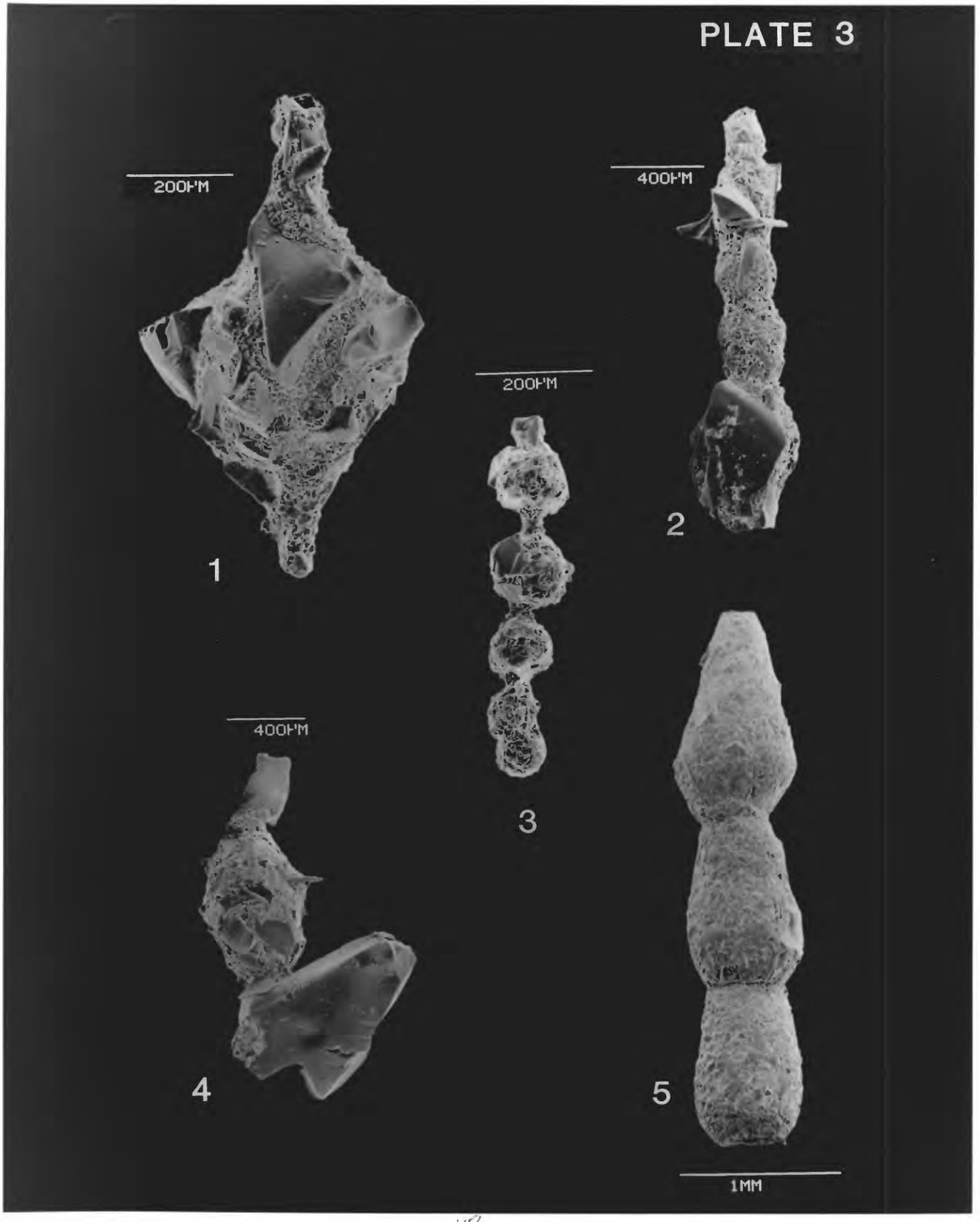

PLATE 4

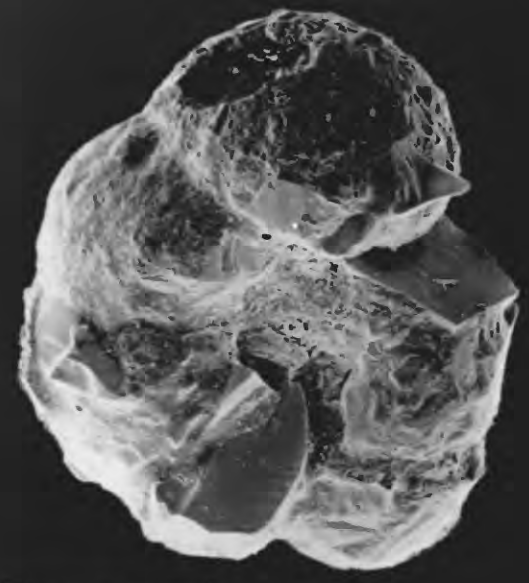

1

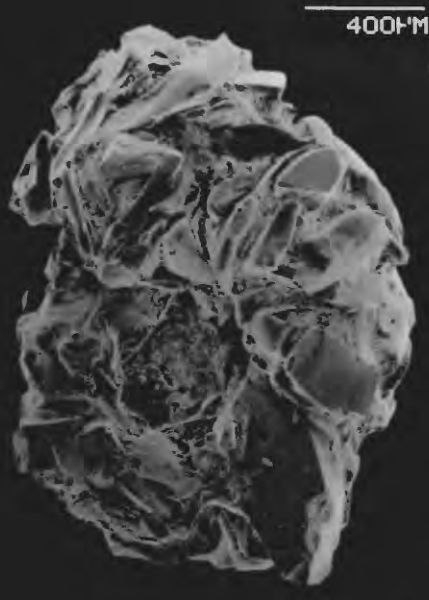

2

3

4